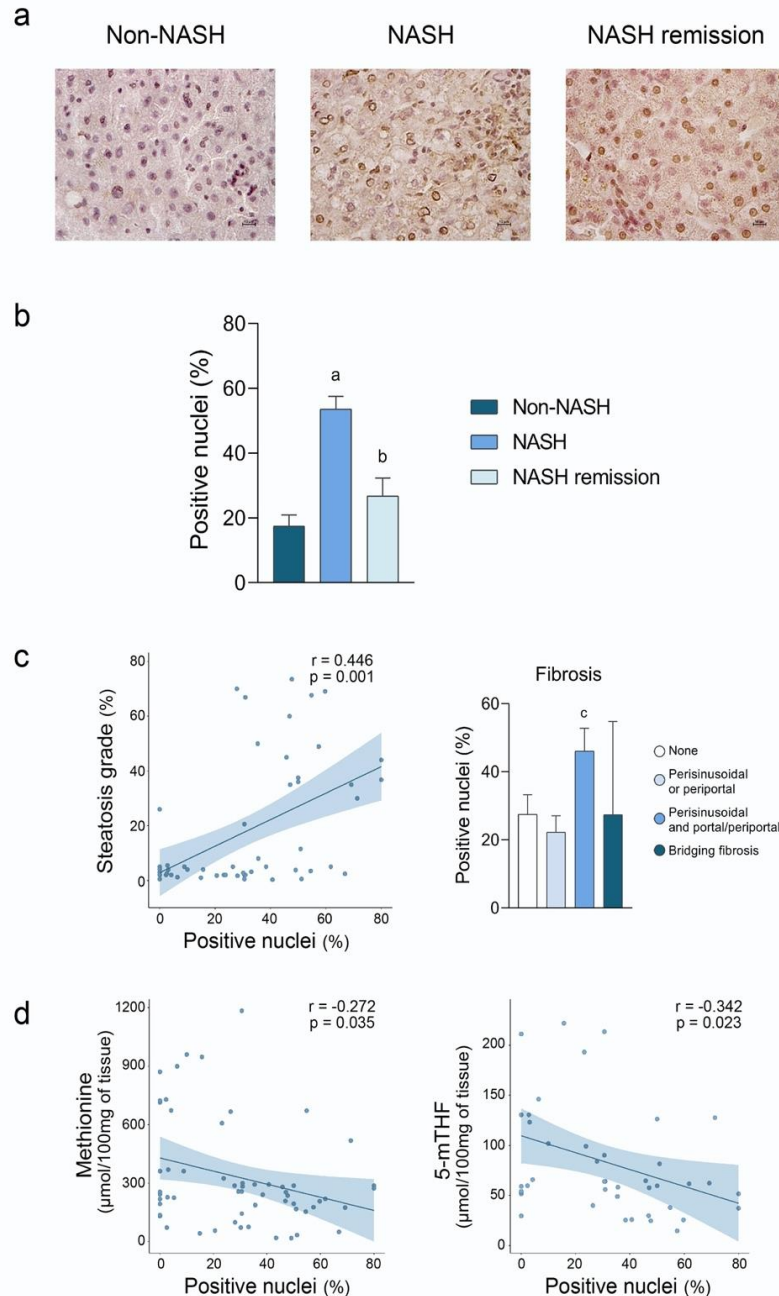
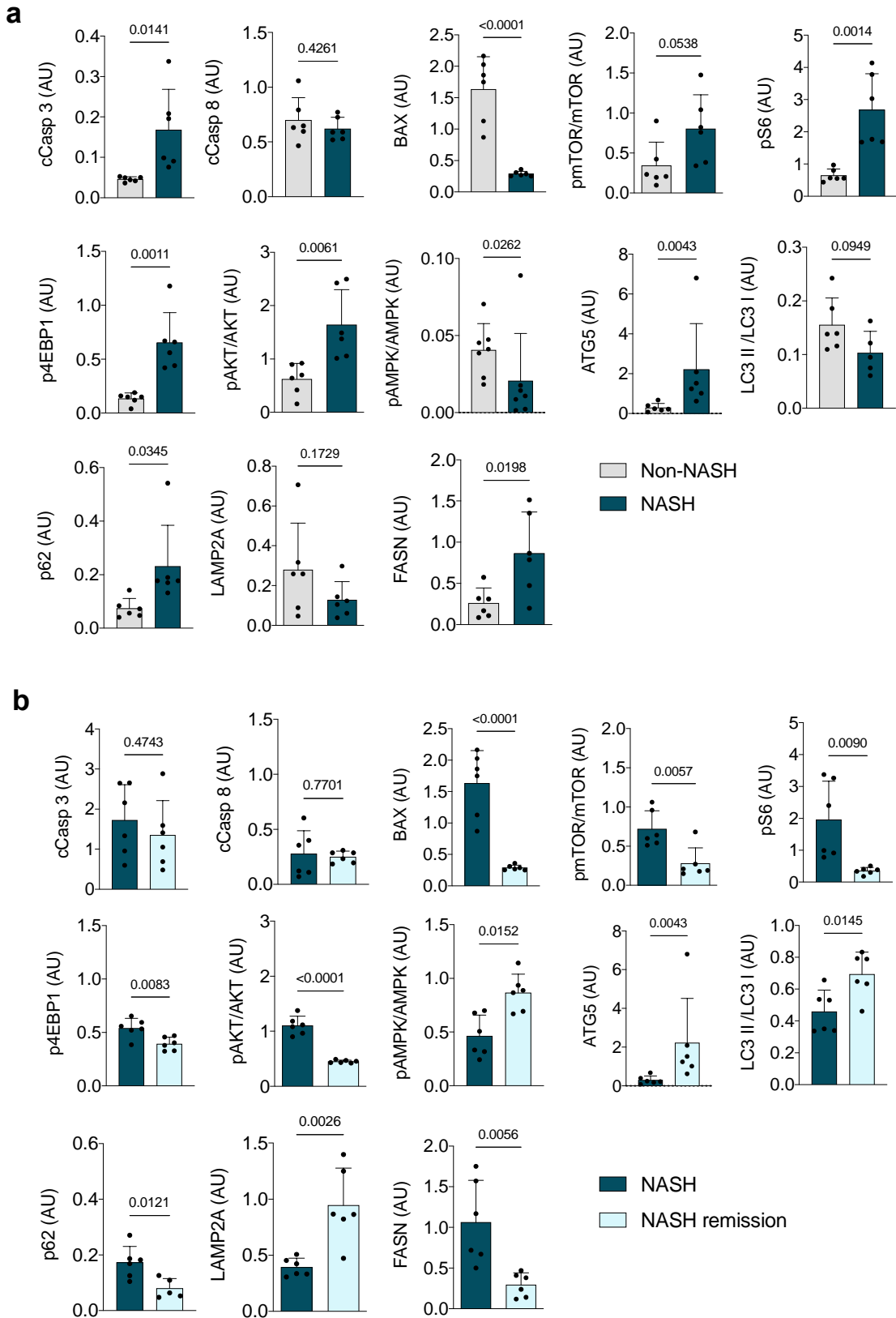


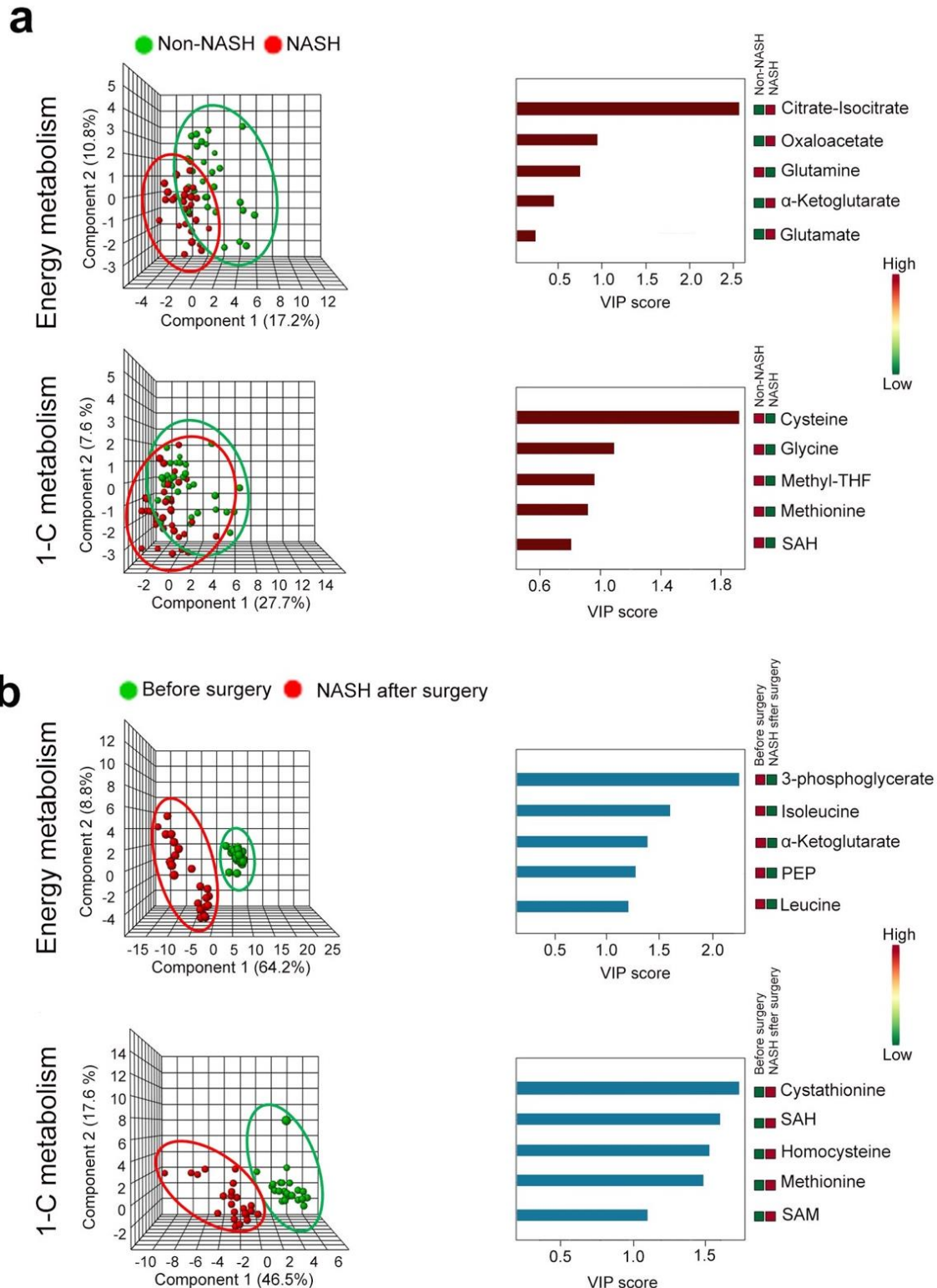
Supplementary Figure S1. NASH remission is associated with reduced liver mitochondrial damage, oxidative stress and inflammation. Western blot quantification for selected markers in the livers of patients with and without NASH and patients with NASH before and after surgery. P-values were calculated by the Mann-Whitney U test. Results are shown as means and SD.



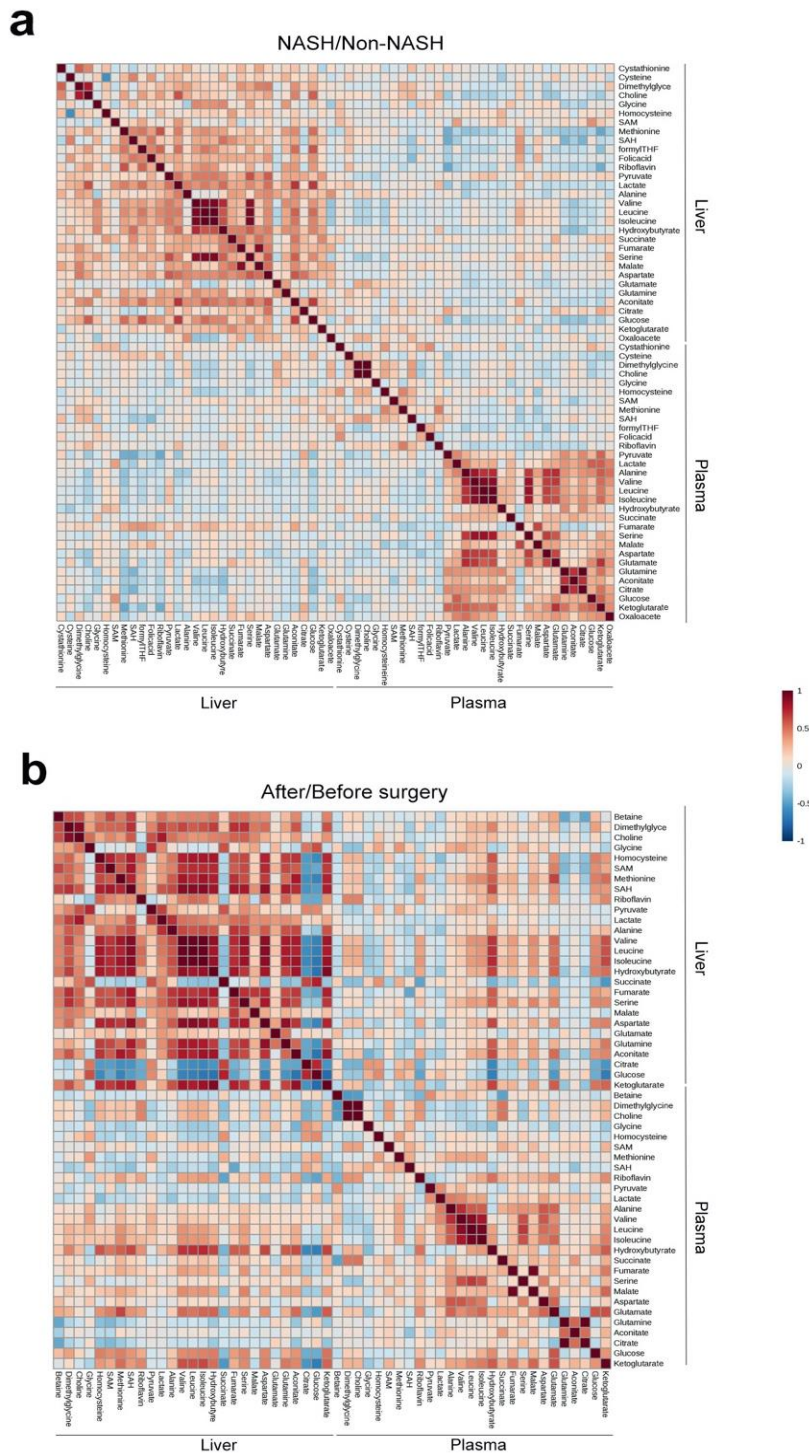
Supplementary Figure S2. Terminal deoxynucleotidyl transferase-mediated dUTP nick end labelling (TUNEL) for the measurement of apoptotic nuclei. (a) Representative micrographs corresponding to liver biopsies from a patient without NASH and 3.1% positive nuclei, a patient with NASH and 71.3% positive nuclei, and a post-surgery biopsy with 25.3% positive nuclei. Nuclei with positive staining appear brown. (b) Patients with NASH showed a significant increase in the proportion of nuclei positive for TUNEL compared to patients without NASH. These values decreased after surgery. (c) The proportion of TUNEL positive nuclei significantly correlated with the steatosis grade and was higher in patients with perisinusoidal and portal/periportal fibrosis. (d) The proportion of TUNEL positive nuclei showed inverse significant correlations with hepatic methionine and 5-methyl tetrahydrofolate (5-mTHF) concentrations. ^a at least $p<0.05$ with respect to patients without NASH; ^b at least $p<0.05$ with respect to patients with NASH; ^c at least $p<0.05$ with respect to patients without fibrosis or perisinusoidal or periportal fibrosis. P-values were calculated by the Mann-Whitney U test. Results are shown as means and SD. Correlations were calculated with the Spearman's rho test.



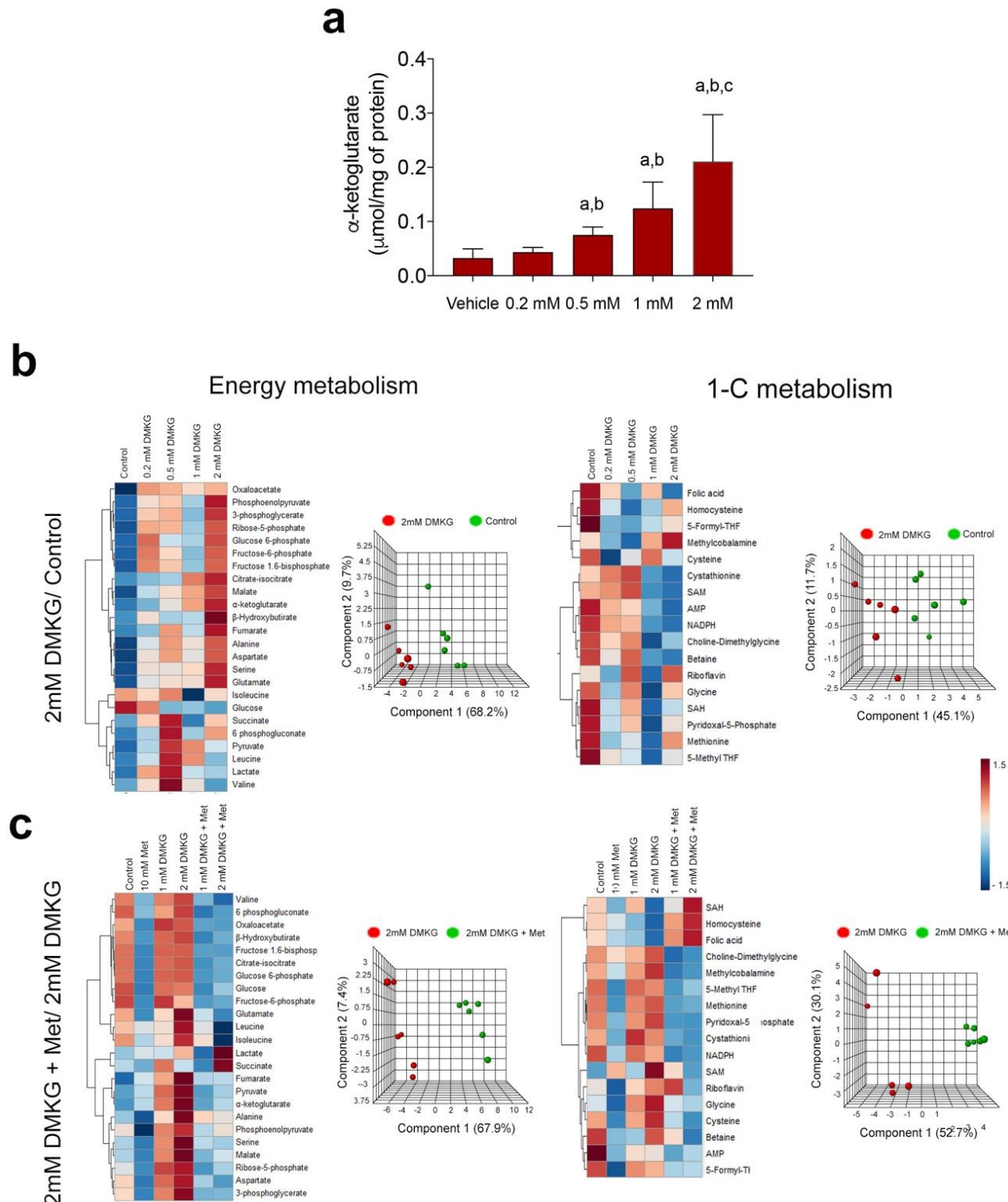
Supplementary Figure S3. mTORC1 signalling and NASH remission. Western blot quantification for selected markers in the livers of patients with and without NASH (a) and NASH patients before and after surgery (c). P-values were calculated by the Mann-Whitney U test. Results are shown as means and SD.



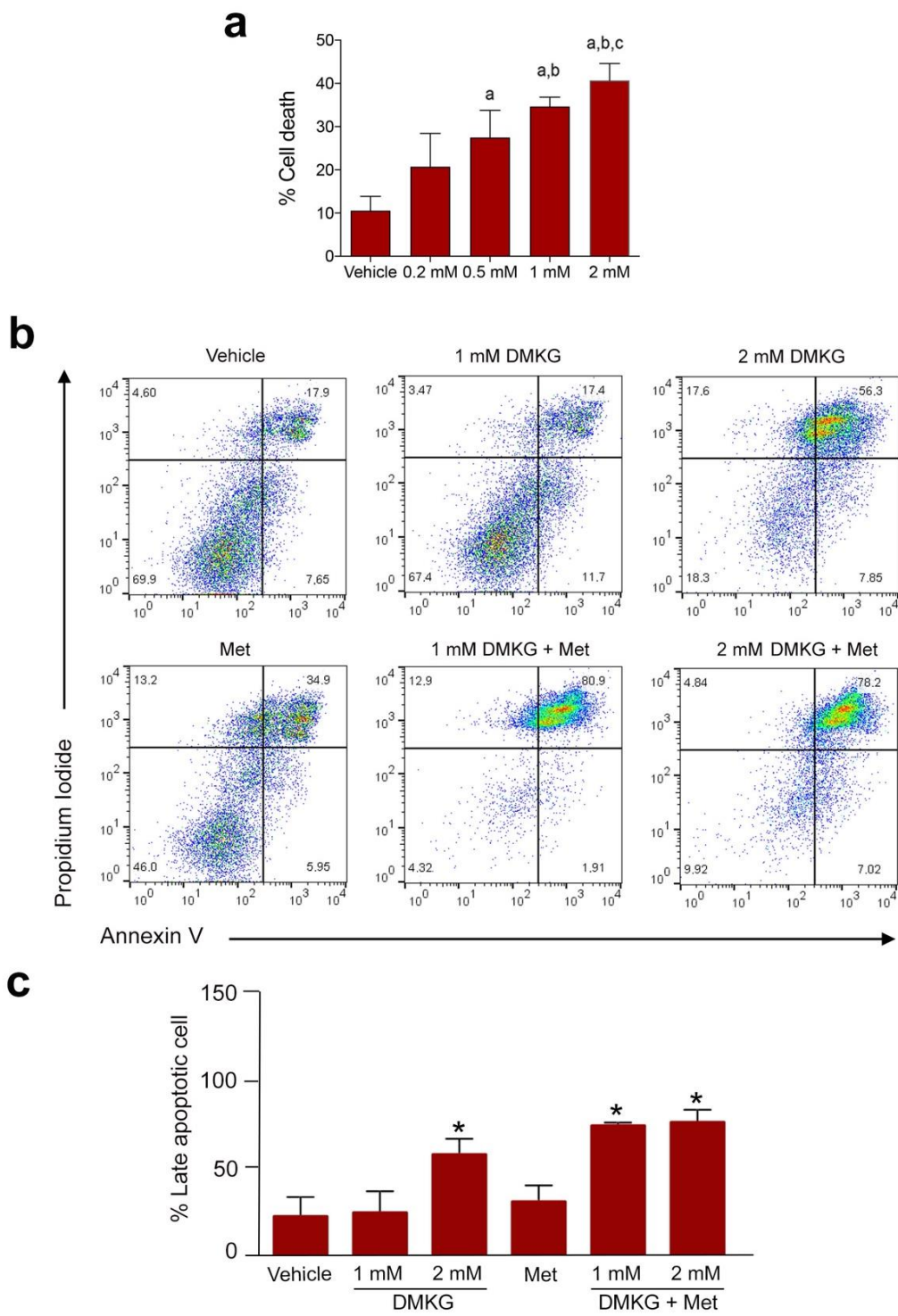
Supplementary Figure S4. Energy and one-carbon metabolism distinguished livers of patients with and without NASH: the effect of NASH remission. (a) Principal component analysis and variable importance scores in random forests indicated the relative importance of different metabolites in distinguishing the livers of patients with and without NASH. (b) The same analyses retained the importance of α -KG-related metabolites and metabolites from the methionine cycle in metabolic reversal after NASH remission.



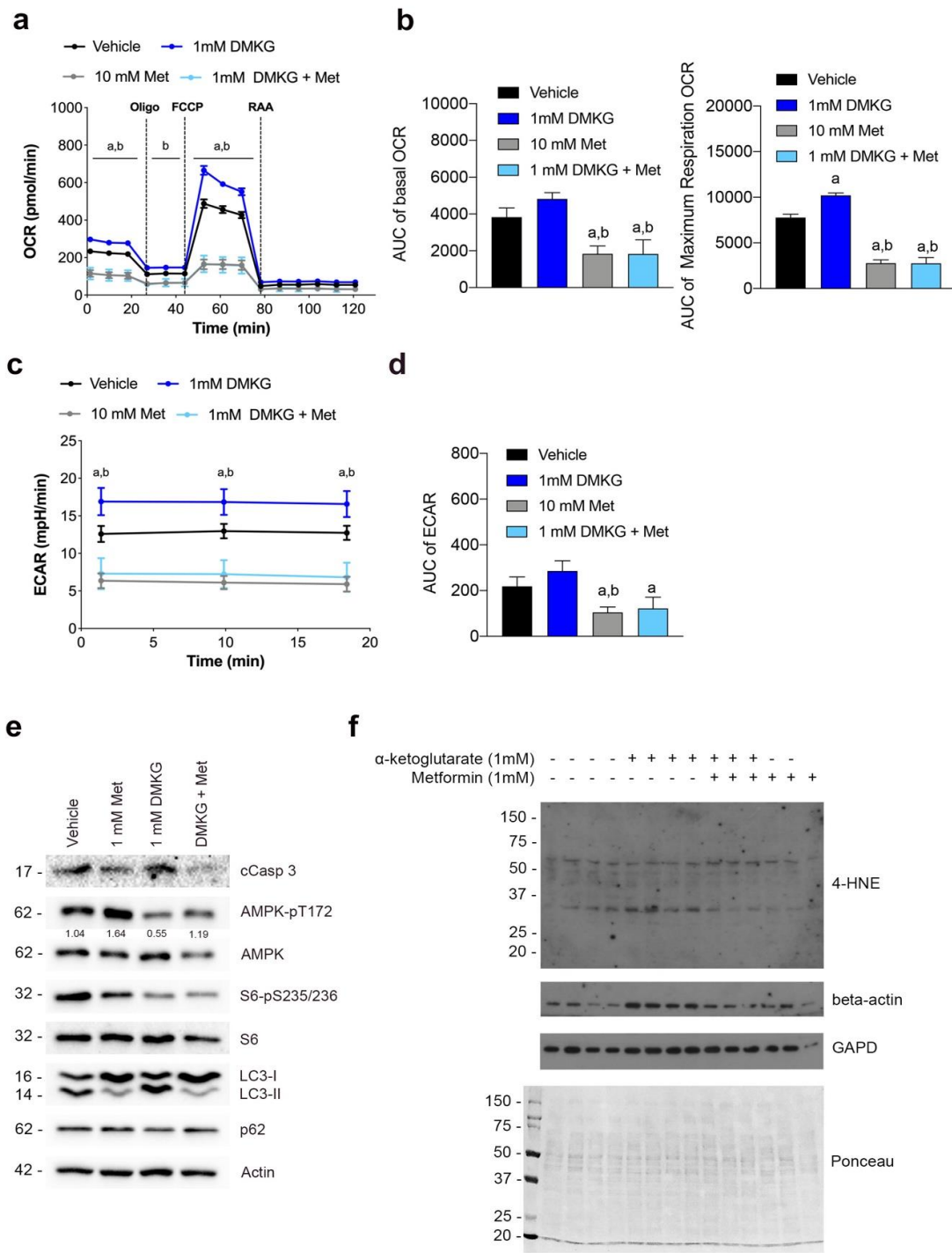
Supplementary Figure S5. The reliability of plasma measurements compared with the liver metabolome. Assessment of the reliability of linear regression estimates and exploratory factor analysis via a correlation matrix between the plasma and liver metabolites in (a) the livers of patients with and without NASH and (b) variations after NASH remission. Collectively, the data displayed a similar response of the metabolome in the plasma and liver. The effect of plasma fumarate on the levels of numerous liver metabolites appeared to be significant when comparing the livers of patients with and without NASH. Similarly, α -KG, glutamine and hydroxybutyrate in the plasma might be associated with the metabolic response in NASH remission. Spearman's correlation was used to decrease susceptibility to outliers.



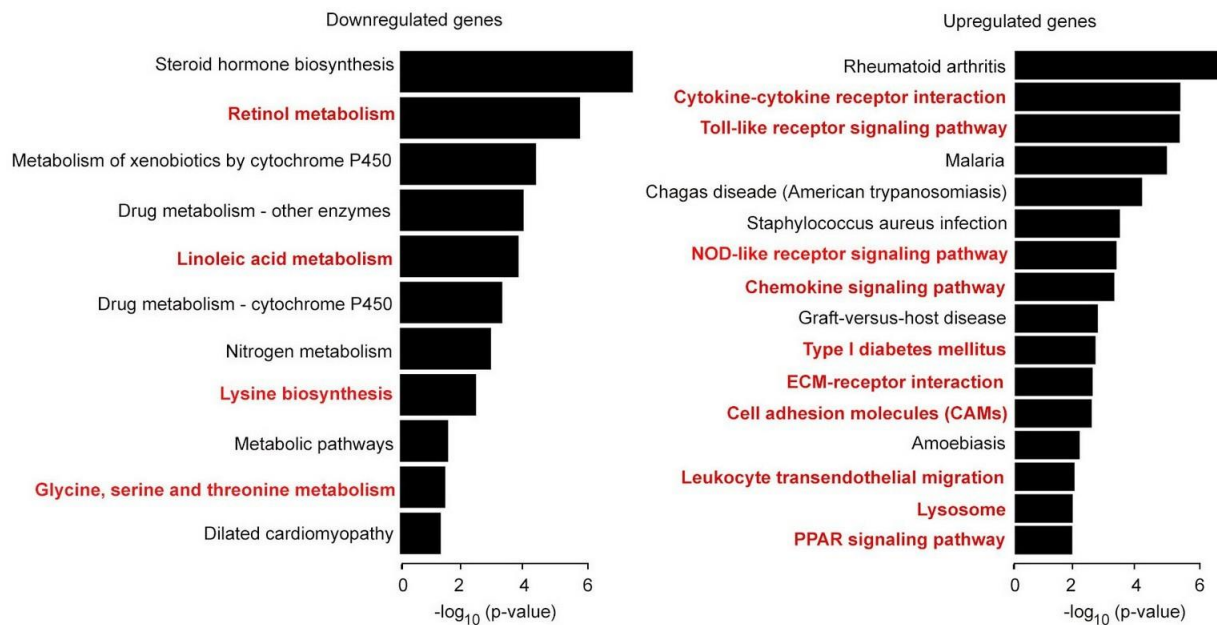
Supplementary Figure S6. Increased hepatocyte α -KG levels affect energy and one-carbon metabolism. (a) Increasing (from 0.2 mM to 2 mM) supplementation with a cell-permeable α -KG analog increased the intracellular α -KG levels. ^aat least $p<0.05$ compared to the controls, ^bat least $p<0.05$ compared to 0.2 mM, ^cat least $p<0.05$ compared to 0.5 mM. (b) Heatmaps and principal component analysis indicated dose-dependent changes in metabolites that distinguished the treated and untreated cells. (c) The addition of metformin abrogated most metabolic changes induced by α -KG supplementation. P-values are calculated by the Mann-Whitney U test. Results are shown as means and SD.



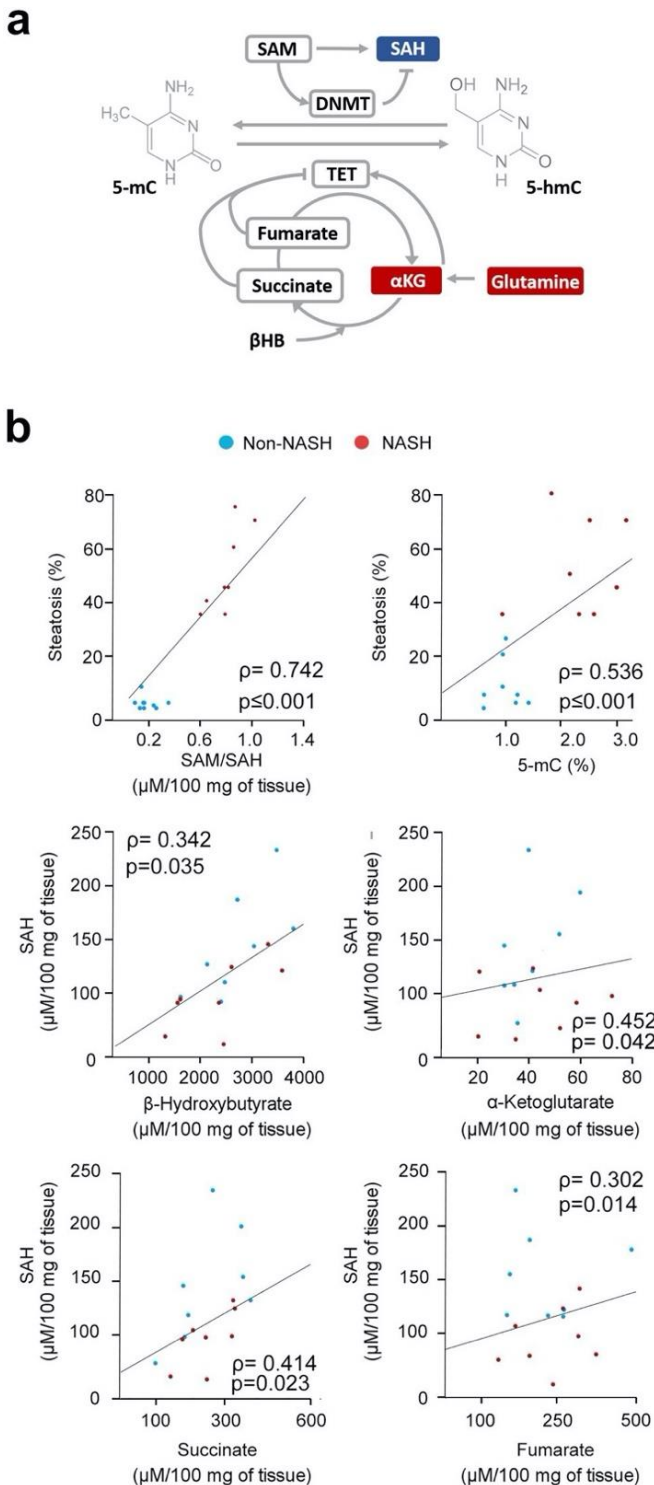
Supplementary Figure S7. Increased hepatocyte α -KG levels promote death in cultured hepatocytes. (a) Increasing (from 0.2 mM to 2 mM) supplementation with a cell-permeable α -KG analog increased cell death. ^aat least $p<0.05$ compared to controls, ^bat least $p<0.05$ compared to 0.2 mM, ^cat least $p<0.05$ compared to 0.5 mM. (b) Flow cytometry analysis of the cells stained with annexin V and propidium iodide indicated an increase in apoptosis caused by high intracellular α -KG levels. (c) The number of late apoptotic cells confirmed that metformin may potentiate the effect of high α -KG levels. Results expressed as mean \pm s.e.m. p values are determined by Wilcoxon rank-sum test (a) or * $p<0.05$ (ANOVA post hoc Bonferroni test in quintuplicate) in (c).



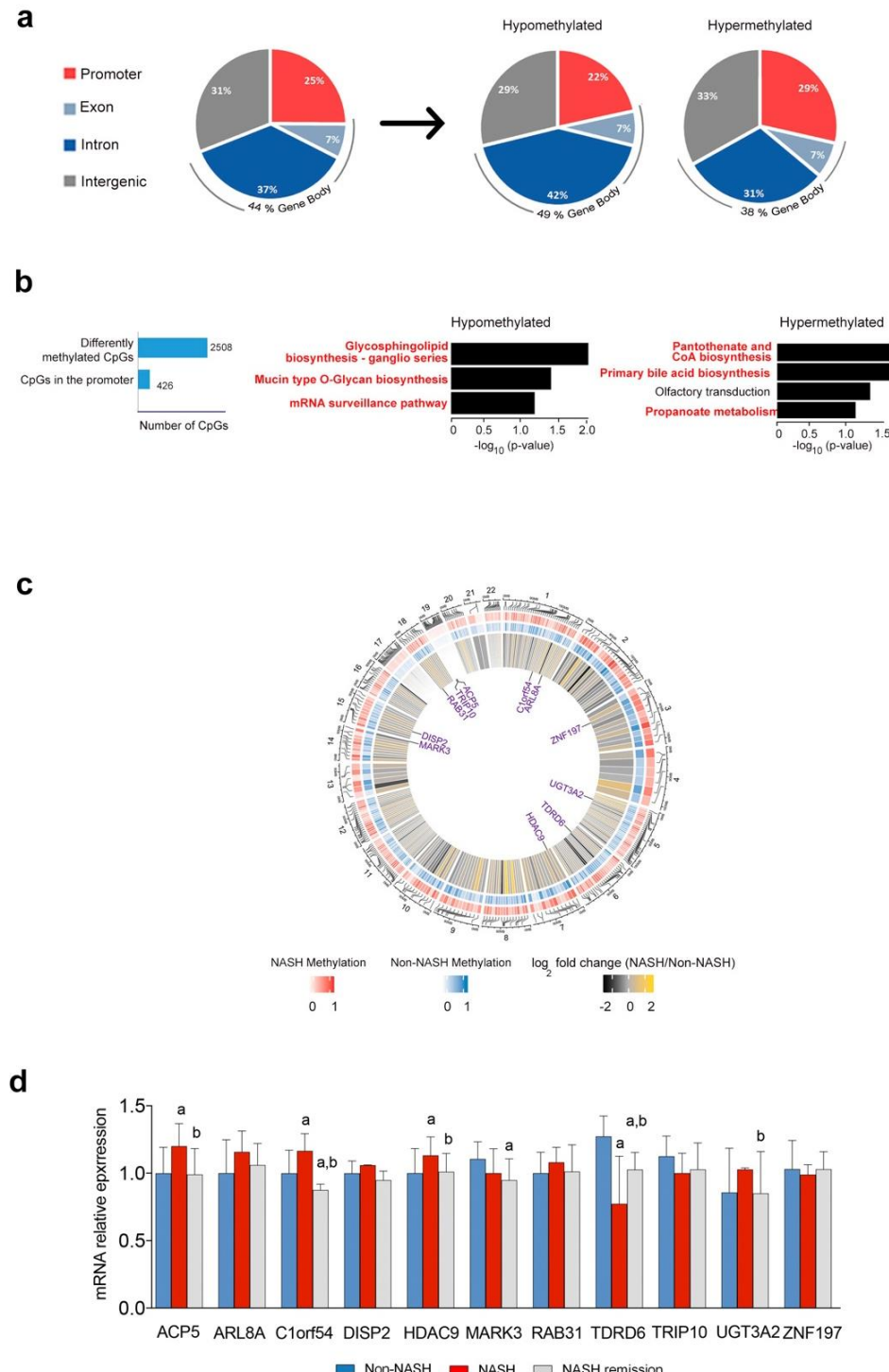
Supplementary Figure S8. Metformin regulates mitochondrial function in primary hepatocytes cells. (a,b). Oxygen consumption rate (OCR) and (c,d) extracellular acidification rate (ECAR) of primary hepatocytes cells revealed that supplementation with metformin abrogated α -KG-induced key cellular functions, as mitochondrial respiration and glycolysis. (e) Representative western blots of selected markers indicated that metformin also abolishes these effects by increasing AMPK phosphorylation. (f) Representative western blots of 4-hydroxynonenal (4-HNE) showed that the increase of intracellular α -KG did not alter the oxidative stress in the primary hepatocytes cells. ^a at least $p<0.05$ compared to control, ^b at least $p<0.05$ compared to 1 mM DMG, ^c at least $p<0.05$ compared to 10 mM metformin. Results expressed as mean \pm s.e.m. p values are determined by One or two -way ANOVA with Tukey's posthoc test.



Supplementary Figure S9. KEGG pathway analysis of NASH and non-NASH phenotypes. The functional annotation of differentially expressed genes (upregulated and downregulated on the right and left, respectively) between patient cohorts indicated an association with biological processes involved in metabolism and disease.

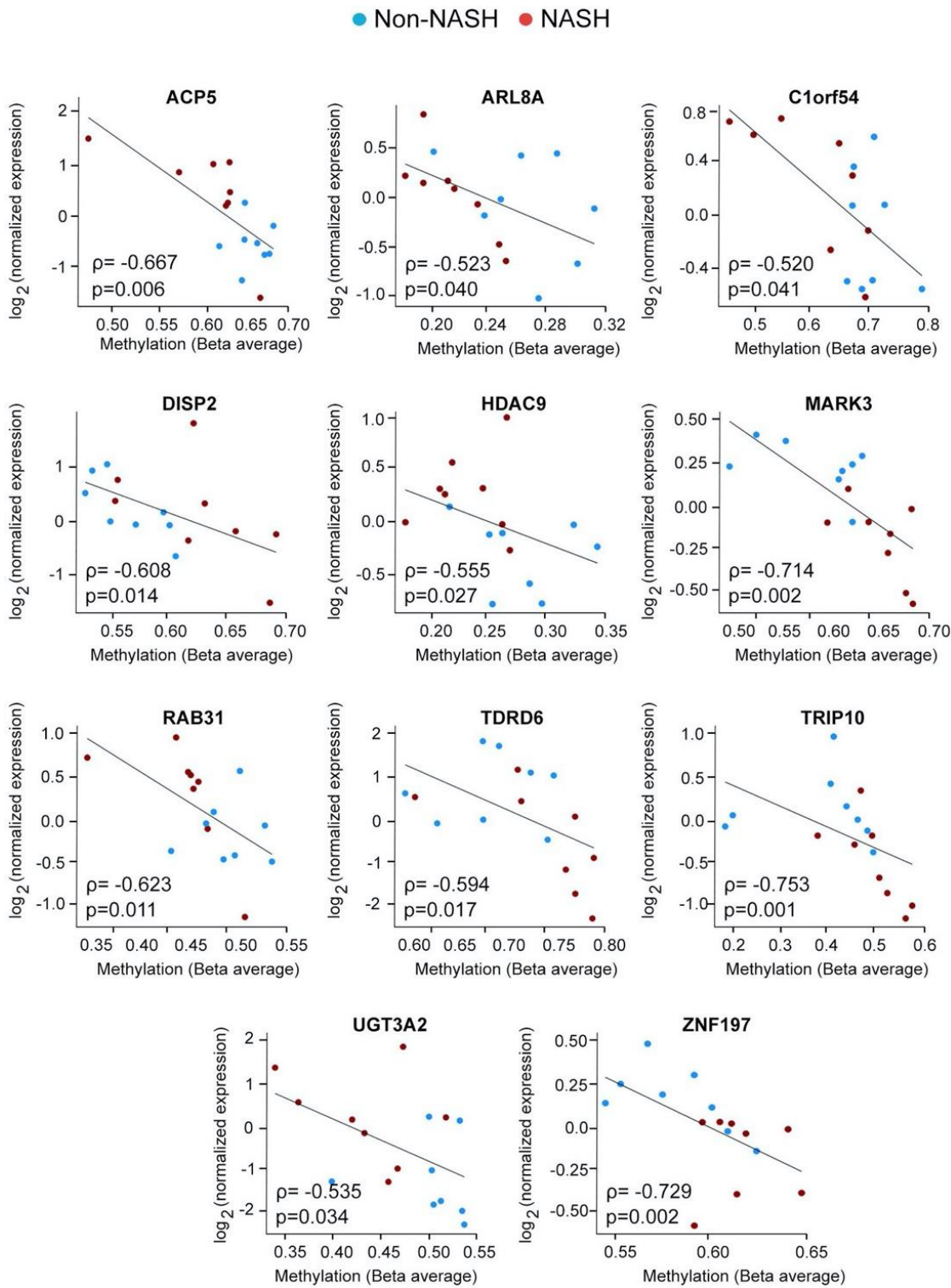


Supplementary Figure S10. Metabolites influence DNA methylation. (a) Several families of enzymes affect DNA methylation and require methyl donors and/or relative concentrations of mitochondrial metabolites. (b) Steatosis correlated with the amount of methyl donors and 5-methylcytosine. Hepatic mitochondrial metabolites are interrelated and distinguished the livers of patients with and without NASH. Correlations were calculated with the Spearman's rho test



Supplementary Figure S11. Methylated CpG sites in livers of patients with NASH are not uniformly distributed in the genome.

(a) Overall distribution of significantly differentially methylated CpG sites in promoter, exon, intron and intergenic regions indicated as percentages. (b) KEGG pathway analysis of gene expression in hypo- and hypermethylated promoter regions. Of the 2508 differentially methylated CpGs from the experiment, 426 are localised to promoters (we filtered for those annotated as TSS1500 or TSS200), as summarised in the blue bar chart on the left. (c) Circos plot showing chromosome locations of the subset of 367 CpGs for which we have mRNA microarray data (of the 426 from (b)) from Figures 7 and S8, with red and blue layers indicating localization and methylation levels in NASH and Non-NASH patients, respectively. The interior layer shows \log_2 (fold-change) in mRNA levels between NASH and Non-NASH patients, and text labels indicate CpGs highlighted in purple in Figure 7e. (d) Transcriptome response in selected genes using quantitative real-time PCR. ^a At least $p<0.05$ compared to non-NASH livers, ^b at least $p<0.05$ compared to NASH livers. Results expressed as means and SD. p values are determined by Wilcoxon rank-sum test.



Supplementary Figure S12. Representative DNA methylation and mRNA expression measured in candidate CpG sites located in promoter regions. Spearman's correlation plots of DNA methylation (beta average) versus gene expression (\log_2 expression) in the livers of patients with and without NASH for the 11 candidates with inverse correlation between DNA methylation and mRNA expression. p-values determined by Spearman cor.test() in R. ACP5, acid phosphatase 5, tartrate-resistant; ARL8A, ADP ribosylation factor-like GTPase 8A; C1orf54, chromosome 1 open reading frame 54; DISP2, dispatched RND transporter family member 2; HDAC9, histone deacetylase 9; MARK3, microtubule affinity-regulating kinase 3; RAB31– RAB31, member RAS oncogene family; TDRD6, tudor domain-containing 6; TRIP10, thyroid hormone receptor interactor 10; UGT3A2, UDP glycosyltransferase family 3 member A2; ZNF197, zinc finger protein 197.

Supplementary Figure S13. Uncropped western blots corresponding to the main figures. M: Western blot protein marker. The numbers to the left of the blots are the molecular weights.

Figure 1b

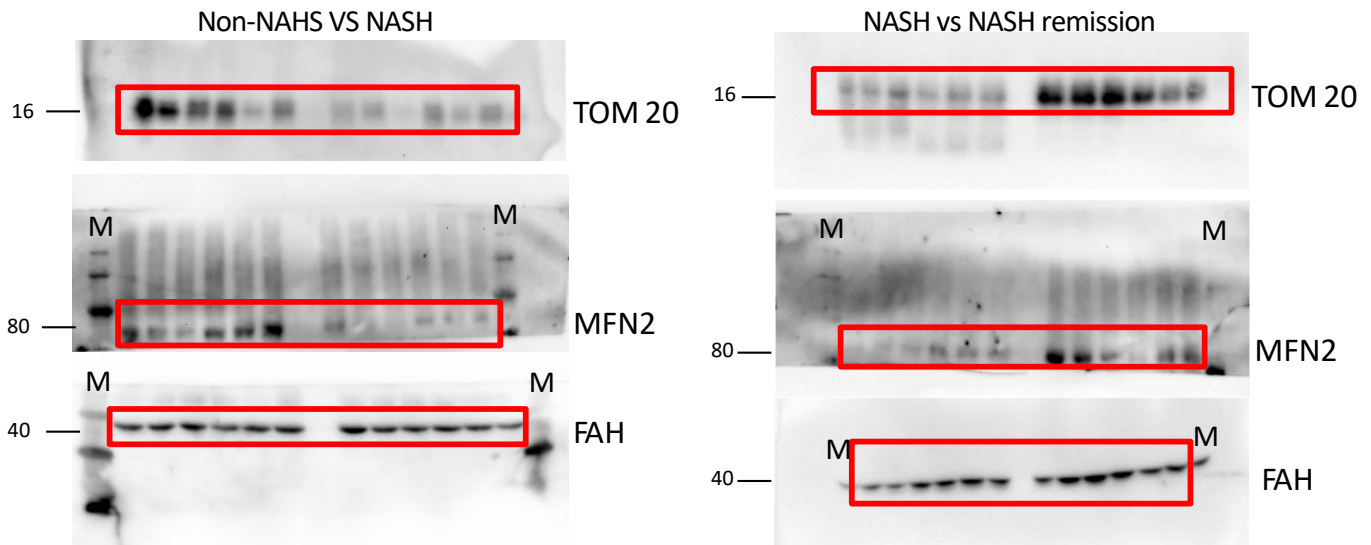


Figure 1c

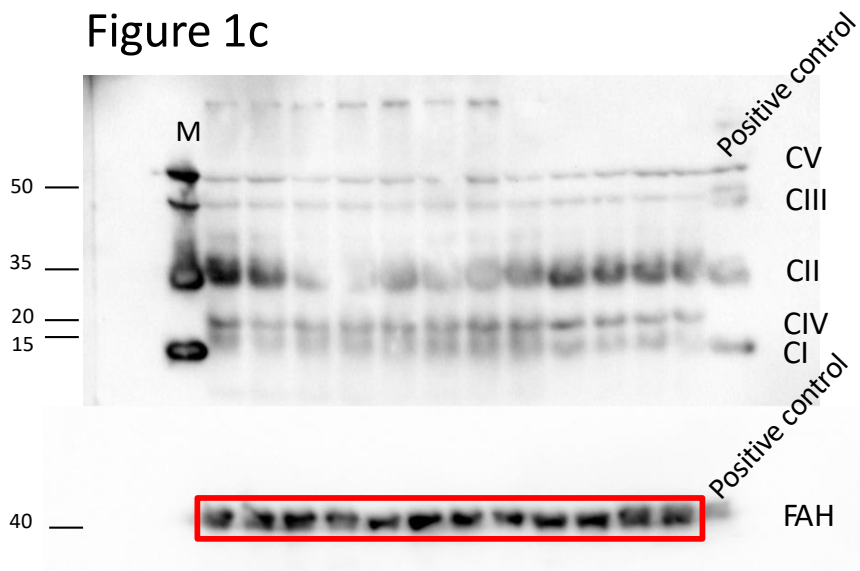


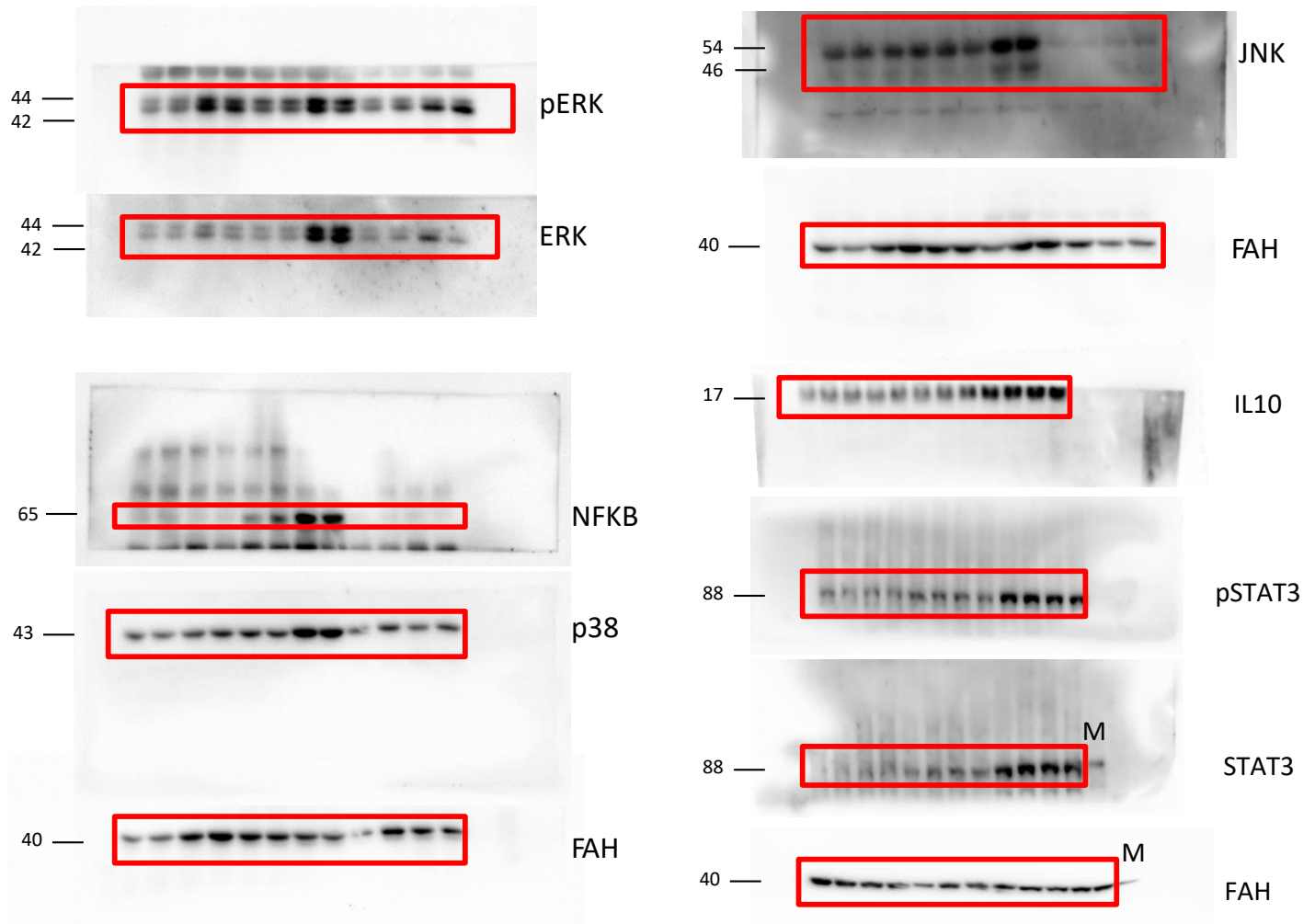
Figure 2b

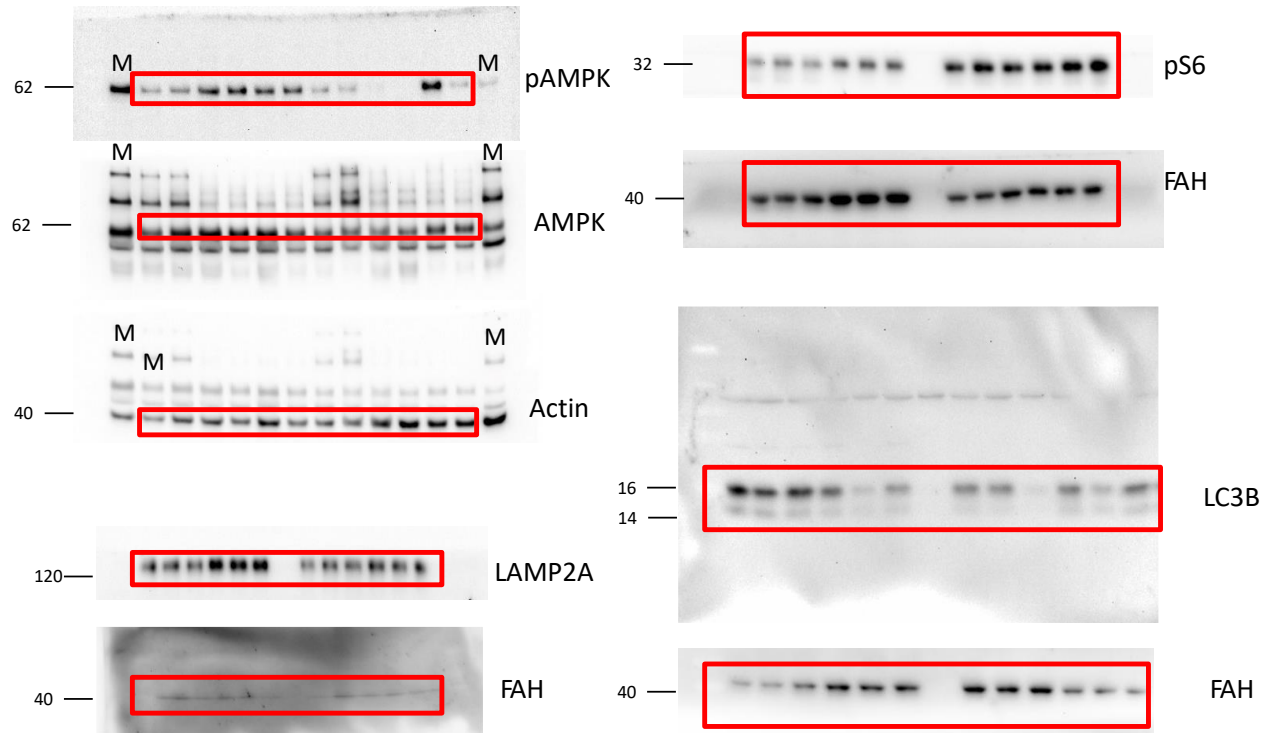
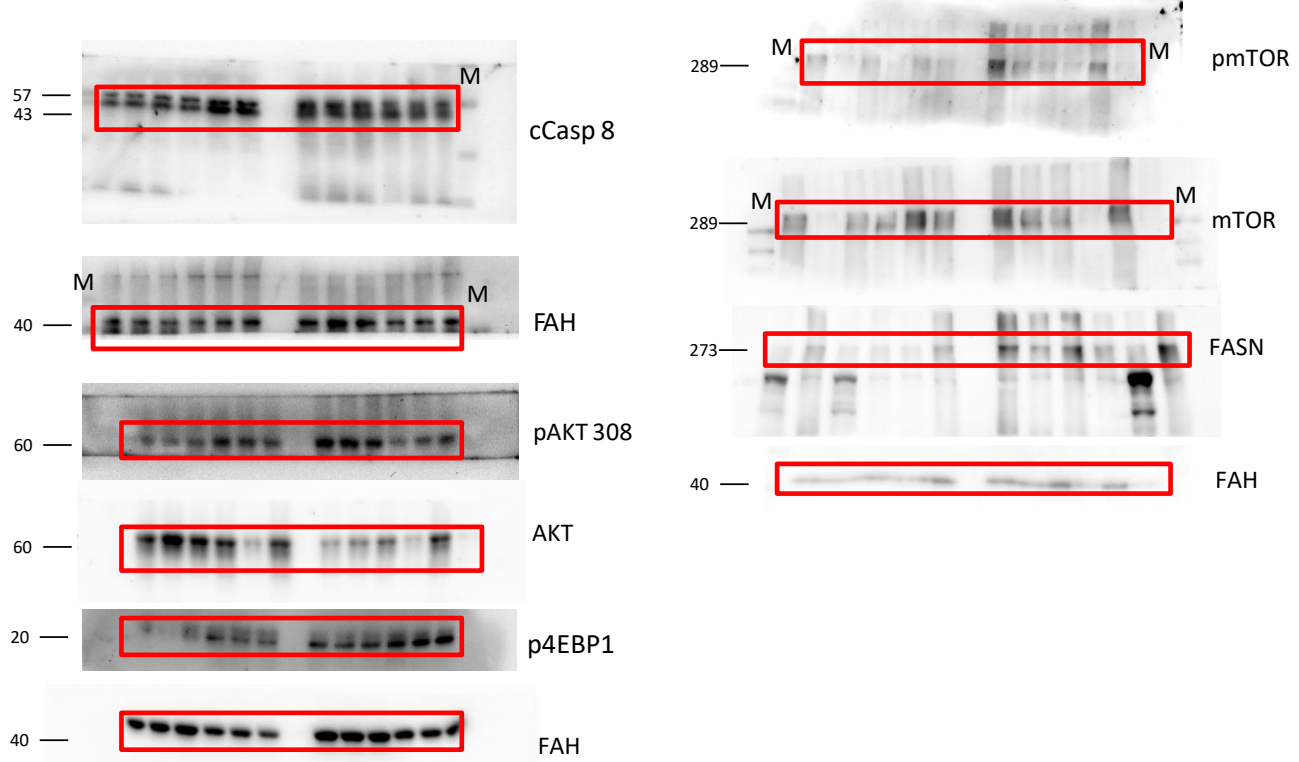
Figure 3B**Figure 3B**

Figure 3B

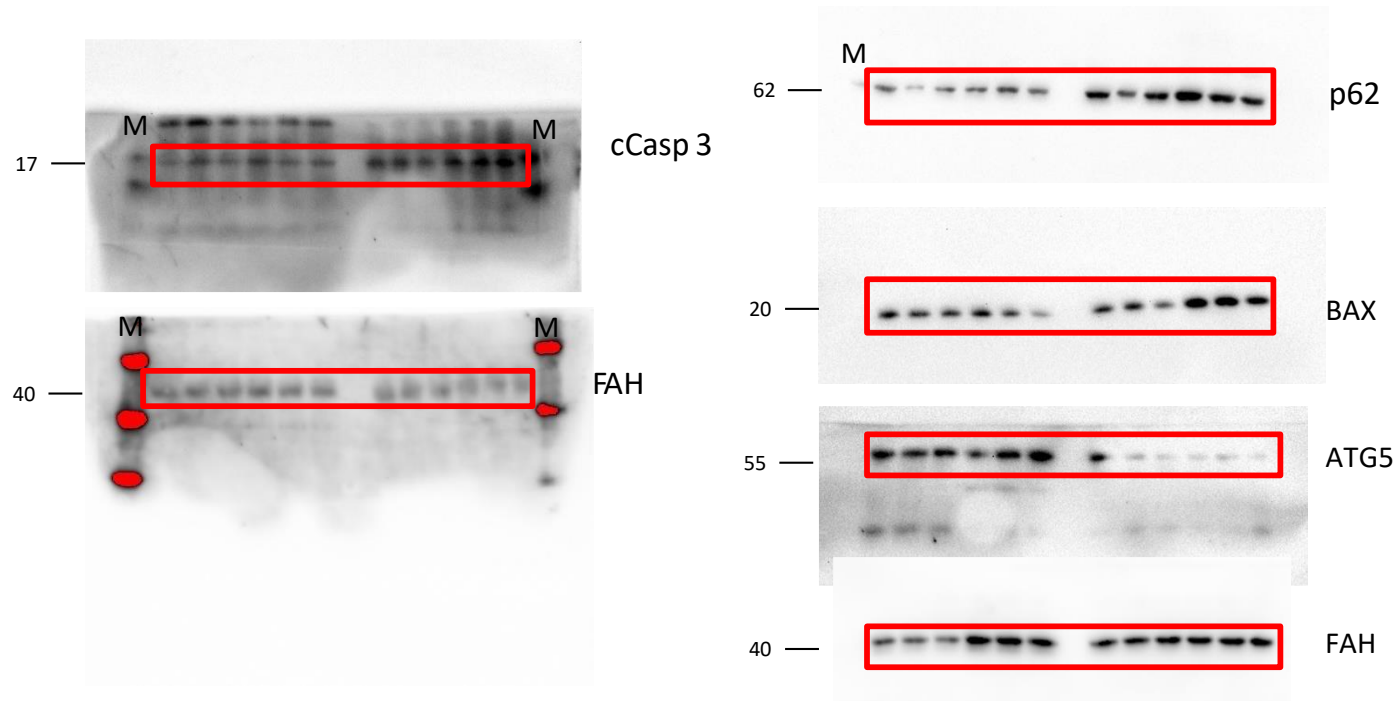


Figure 3D

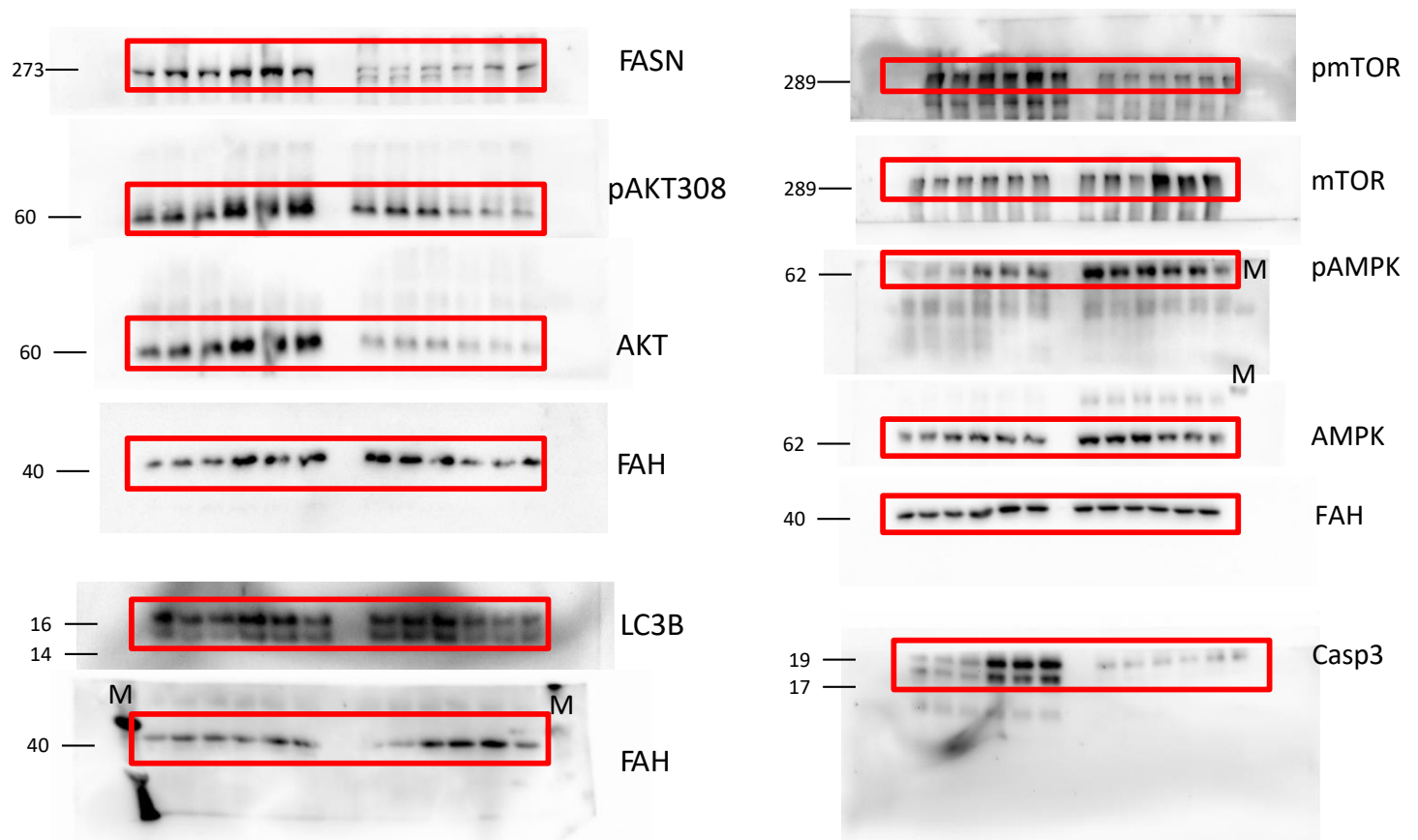


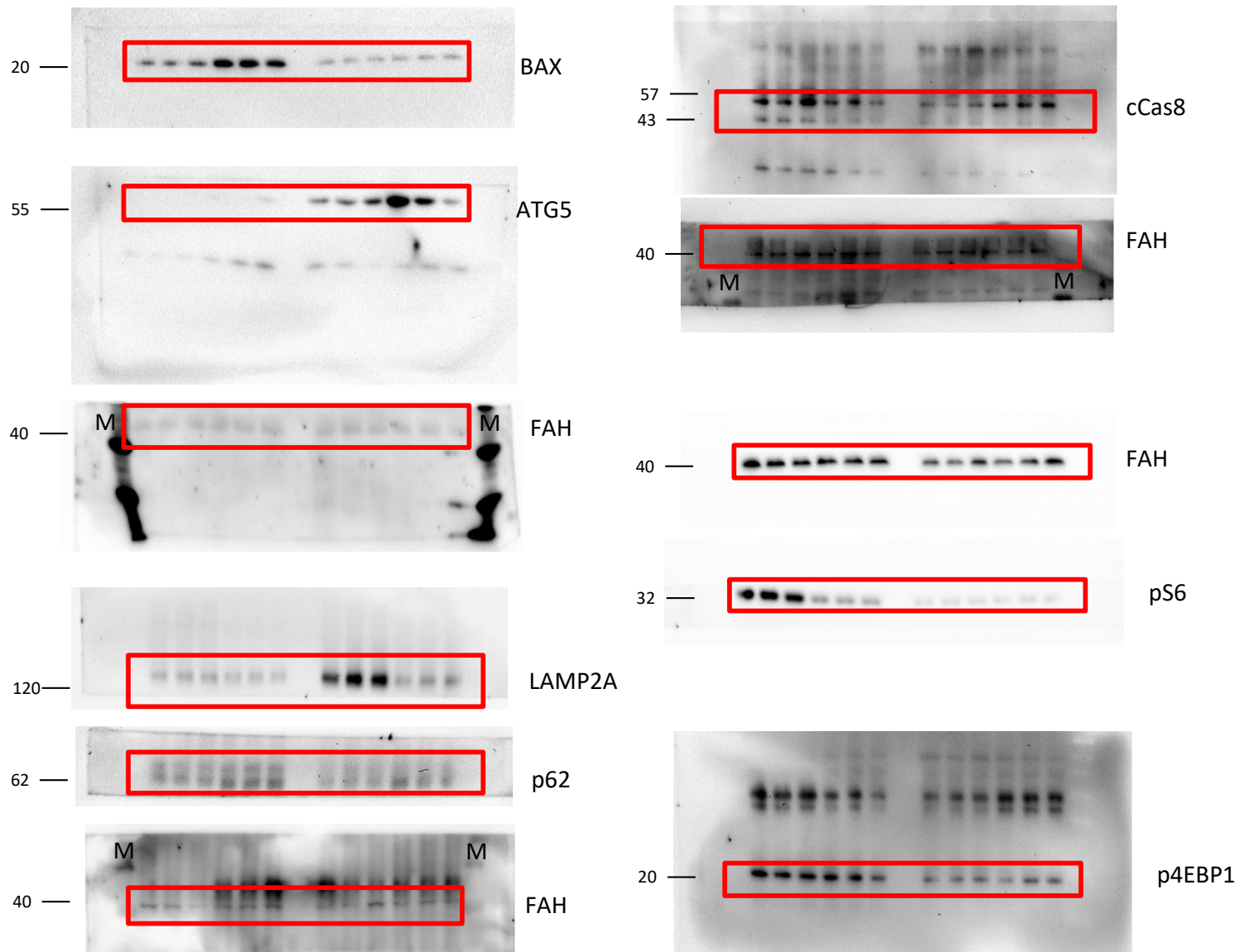
Figure 3D

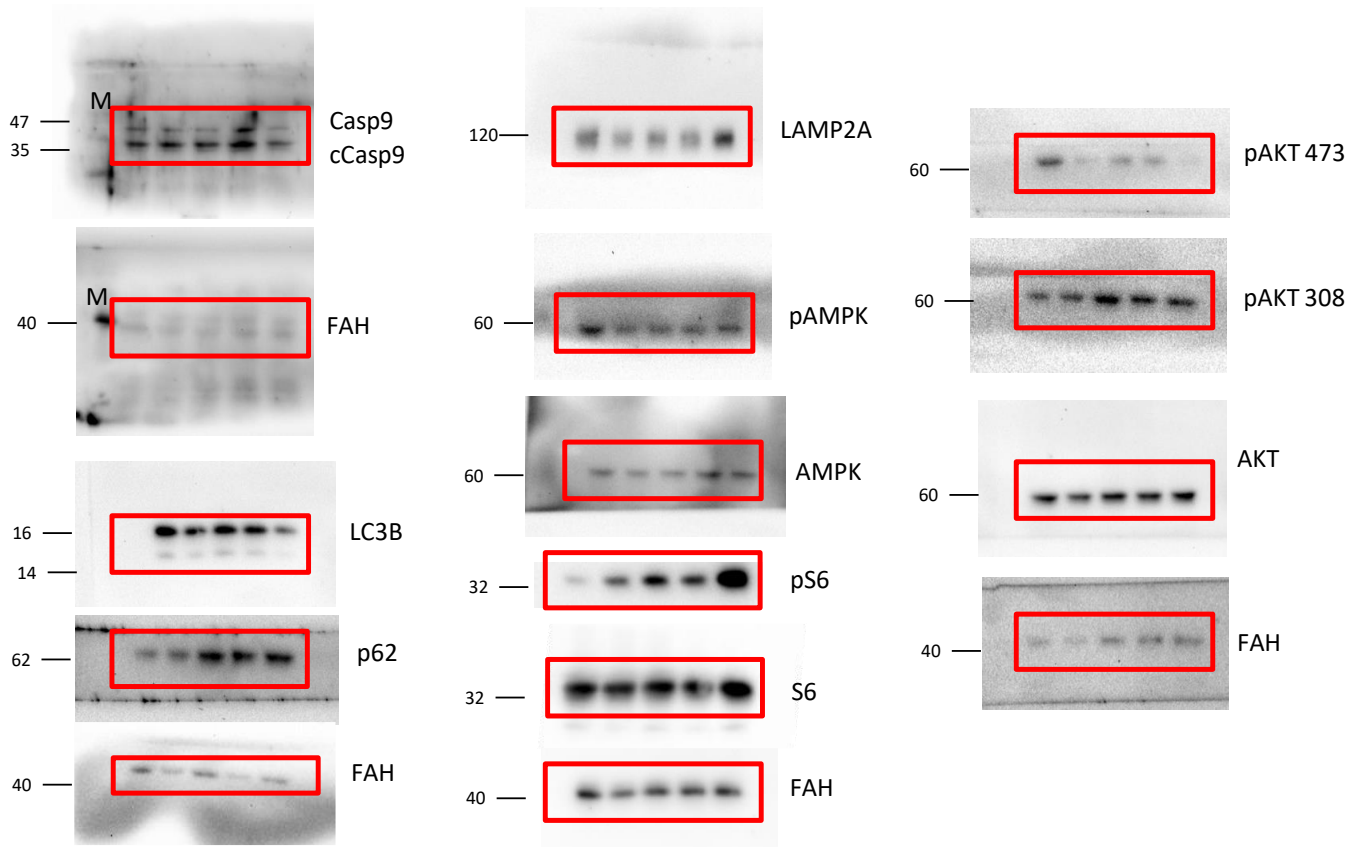
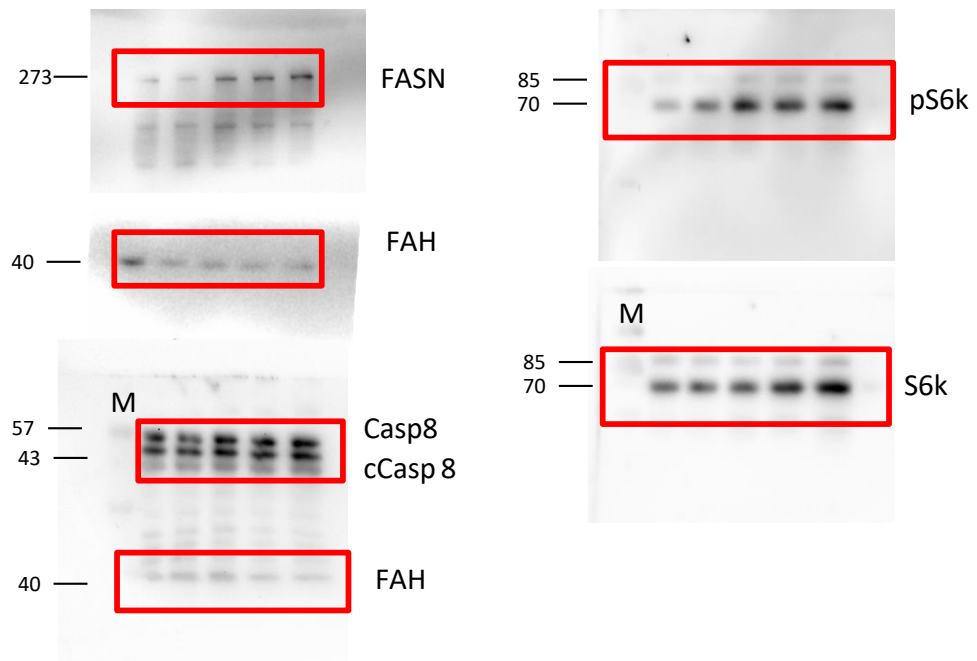
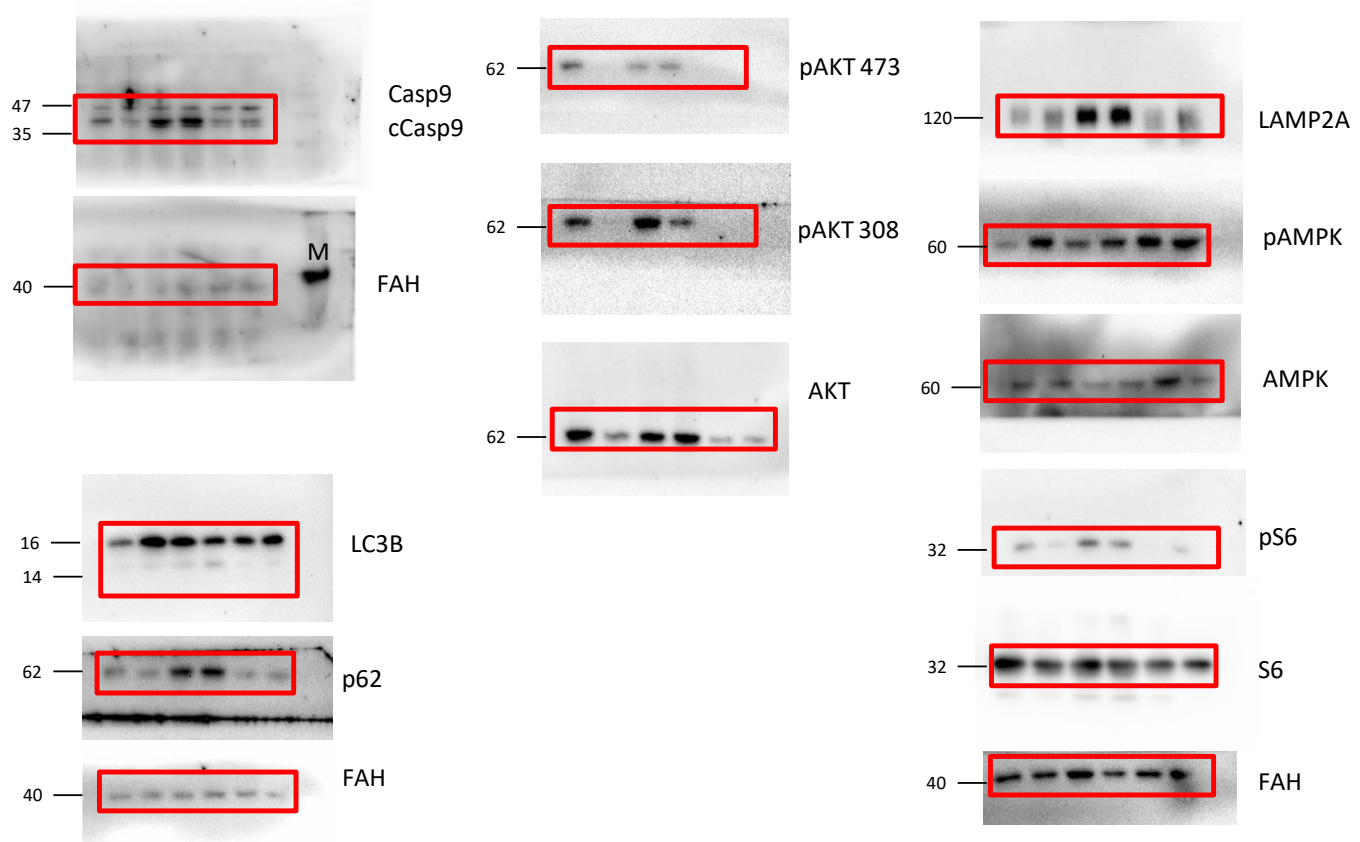
Figure 5c**Figure 5c**

Figure 5d**Figure 5d**

Supplementary Table S1. Clinical, laboratory assessment and liver histological features in patients with severe obesity comparing matched patients with and without NASH. NASH patients were reexamined one year after surgery

	Non-NASH (NAS ≤ 2) (n=31)	NASH (NAS ≥ 5) (n=31)	One-year after surgery (n=31)
Clinical characteristics			
Male, n (%)	10 (32·3)	10 (32·3)	-
Age, years	46·0 (39·0-56·0)	49·0 (44·0-56·0)	-
BMI, Kg/m ²	44·0 (41·4-46·4)	46·5 (42·6-53·6)	31·4 (28·7-33·4) ^{b,c}
T2DM, n (%)	11 (35·5)	17 (54·8)	4 (12·9) ^{b,c}
Hypertension, n (%)	17 (54·8)	21 (67·7)	10 (32·3) ^{b,c}
Dyslipidaemia, n (%)	9 (29·0)	12 (38·7)	2 (6·5) ^{b,c}
Medication (%)			
Metformin	4 (12·9)	12 (38·7) ^a	4 (12·9) ^{b,c}
Insulin	2 (6·5)	5 (16·1)	1 (3·2) ^{b,c}
Sulfonylureas	1 (3·2)	2 (6·5)	-
ACEIs + ARA-II	11 (35·5)	14 (45·2)	4 (12·9) ^{b,c}
Diuretics	4 (12·9)	5 (16·1)	-
Statins	5 (16·1)	5 (16·1)	2 (6·5) ^{b,c}
Laboratory assessment			
Hemoglobin, g/dL	13·2 (12·7-14·7)	13·4 (12·7-14·8)	13·1 (12·3-14·0)
Leukocytes, x10 ⁹ /L	7·5 (6·3-9·4)	7·6 (6·5-10·7)	6·0 (5·0-7·5) ^c
Platelets, x10 ⁹ /L	197 (187-266)	243 (181-314)	227 (209-251)
Ferritin, µg/L	44·4 (25·0-143·7)	112·4 (31·2-203·3)	32·2 (12·2-85·5) ^{b,c}
Total-cholesterol, mmol/L	4·3 (3·4-5·2)	4·3 (3·8-5·0)	4·8 (4·1-5·4)
HDL-cholesterol, mmol/L	1·2-0·9-1·6)	1·2 (0·9-1·4)	1·5 (1·3-1·7) ^c
LDL-cholesterol, mmol/L	2·4 (1·9-2·8)	2·6 (2·4-3·7) ^a	2·8 (2·3-3·3)
Triglycerides, mmol/L	1·5 (1·0-2·3)	1·7 (1·3-2·5) ^a	0·9 (0·6-1·4) ^{b,c}
Glucose, mmol/L	6·5 (6·1-8·9)	7·6 (6·2-8·7) ^a	4·5 (4·3-5·1) ^{b,c}
Insulin, pmol/L	90·9 (28·3-140·3)	108·0 (48·7-143·7) ^a	40·9 (20·9-58·6) ^{b,c}
HOMA-IR	4·1 (1·3-6·3)	6·7 (2·7-8·1) ^a	1·2 (0·6-1·9) ^{b,c}
Albumin, g/L	44·0 (41·0-45·0)	43·0 (41·0-46·0)	42·0 (41·0-44·0)
AST, µkat/L	0·5 (0·4-0·7)	0·7 (0·5-1·3) ^a	0·3 (0·2-0·3) ^{b,c}
ALT, µkat/L	0·5 (0·3-0·7)	0·7 (0·5-1·4) ^a	0·2 (0·2-0·3) ^{b,c}
GGT, µkat/L	0·3 (0·2-0·5)	0·5 (0·3-0·8) ^a	0·2 (0·1-0·5) ^c
CRP, mg/L	0·9 (0·5-1·5)	1·9 (0·6-1·5) ^a	0·4 (0·2-0·4) ^{b,c}
Liver histologic features			
Steatosis			
<5%	27 (87·1)	-	31 (100) ^c
5-33%	3 (9·7)	3 (9·7) ^a	-
34-66%	1 (3·2)	15 (48·4)	-
>66%	-	13 (41·9)	-
Lobular inflammation			
No foci	12 (38·7)	-	24 (77·4) ^{b,c}
<2 foci	16 (51·6)	5 (16·1) ^a	7 (22·6)
2-4 foci	3 (9·7)	21 (67·7)	-
>4 foci	-	5 (16·1)	-
Hepatocellular Ballooning			
None	26 (83·8)	2 (6·5) ^a	31 (100) ^{b,c}
Few cells	5 (16·1)	20 (64·5)	-
Many cells	-	9 (29·0)	-
Fibrosis			
None (F0)	8 (25·8)	4 (12·9)	17 (54·8) ^{b,c}
Perisinusoidal or periportal (F1)	18 (58·1)	8 (25·8)	13 (41·9)
Perisinusoidal and portal (F2)	5 (16·1)	15 (48·4)	1 (3·3) ^{b,c}
Bridging fibrosis (F3)	-	4 (12·9)	-

Values were expressed as number of cases and percentages or medians and interquartile range. ACEIs: Angiotensin-converting-enzyme inhibitor; ALT: Alanine transaminase; AST: Aspartate transaminase; ARA-II: Angiotensin II receptor antagonists; BMI: Body mass index; CRP: C-reactive

protein; HDL: High-density lipoprotein; HOMA-IR: Homeostatic model assessment of insulin resistance; HTG: Hypertriglyceridemia; LDL: Low-density lipoprotein; T2DM: Type 2 diabetes mellitus. Significant differences in comparisons are indicated by ^anon-NASH vs. NASH, ^bNon-NASH vs 12 months after surgery. ^cNASH vs one-year after surgery (at least $p<0.05$) by Wilcoxon rank-sum test.

Supplementary Table S2. Quantitative targeted metabolome in livers with, without NASH and 1 year after surgery from patients with severe obesity

Metabolite	Non-NASH (n=31)	NASH (n=31)	One-year after surgery (n=31)
Energy Metabolism			
α -ketoglutarate	3.5 (2.9 – 4.1)	4.4 (3.4 – 5.1) ^a	0.4 (0.3 – 0.6) ^{b, c}
β -hydroxybutyrate	198.3 (150.5 – 247.9)	170.2 (129.7 – 208.8)	22.5 (20.2 – 27.8) ^{b, c}
Aconitate	5.9 (4.3 – 7.5)	5.9 (4.5 – 6.5)	1.4 (1.0-2.2) ^{b, c}
Alanine	631.7 (545.0 – 692.0)	675.5 (579.3- 727.8)	312.8 (179.8 – 553.0) ^{b, c}
Aspartate	110.8 (73.2 – 128.2)	119.0 (84.9 – 154.7)	29.2 (23.0 – 36.4) ^{b, c}
(Iso)Citrate	0.12 (0.07 – 0.16)	0.17 (0.11 – 0.31) ^a	0.84 (0.6 – 1.2) ^{b, c}
Fructose-1,6BP	9.0 (7.5 – 10.2)	10.1 (8.5 – 10.8)	5.7 (3.5 – 7.5) ^{b, c}
Fructose-6P	15.8 (13.3 – 16.6)	18.1 (15.4 – 19.7) ^a	8.9 (5.7-14.3) ^{b, c}
Fumarate	20.8 (16.3 – 28.6)	21.0 (16.4 – 26.2)	8.4 (4.7 – 10.7) ^{b, c}
Glucose	118.4 (75.6 – 144.8)	103.7 (81.5 – 103.7)	73.6 (37.0 – 90.9) ^{b, c}
Gluconate-6P	9.8 (7.0 – 12.5)	7.7 (5.2 – 9.2) ^a	ND
Glucose-6P	13.7 (11.4 – 15.7)	15.3 (12.9 – 16.5)	25.3 (14.8 – 30.4) ^{b, c}
Glutamate	361.8 (242.2 – 481.8)	493.7 (351.7 – 586.7)	528.1 (359.8 – 761.7) ^b
Glutamine	2212.1 (1818.1 – 2628.4)	2524.5 (1796.4 – 3249.6) ^a	2110.6 (1478.9 – 5212.7) ^{b, c}
Glyceraldehyde-3P	8.3 (5.5 – 10.5)	7.2 (5.9 – 8.7)	ND
Glycerate-3P	33.5 (30.2 – 47.3)	38.4 (31.6 – 54.3)	21.1 (18.5 – 21.8) ^{b, c}
Isoleucine	209.1 (123.0 – 265.8)	208.4 (179.0 – 242.0)	12.1 (8.9 – 26.8) ^{b, c}
Lactate	1057.0 (956.5 – 1380.7)	1085.9 (983.5 – 1212.6)	1121.2 (499.6 – 1833.9)
Leucine	383.3 (245.9 – 503.2)	372.7 (301.1 – 441.6)	37.6 (30.3 – 68.7) ^{b, c}
Malate	42.5 (35.1 – 51.3)	44.6 (34.1 – 58.5)	43.1 (27.0 – 56.0)
Oxolacetate	2.3 (1.5-3.9)	2.8 (1.4-4.6)	ND
Phosphoenolpyruvate	10.1 (7.5 – 15.8)	11.0 (8.7 – 13.7)	2.2 (0.6 – 2.8) ^{b, c}
Pyruvate	7.5 (6.0 – 8.9)	10.8 (6.5 – 16.5) ^a	15.0 (6.6 – 21.0) ^{b, c}
Ribose-5P	12.7 (9.8 – 16.3)	12.3 (11.6 – 12.4)	34.2 (23.2 – 46.4) ^{b, c}
Serine	556.1 (338.2 – 748.9)	625.2 (538.4 – 800.2)	267.2 (155.8 – 379.0) ^{b, c}
Succinate	25.2 (19.9 – 32.3)	25.4 (20.6 – 31.2)	62. (34.5 – 95.0) ^{b, c}
Valine	274.3 (157.2 – 364.1)	254.1 (182.9 – 313.6)	34.0 (20.4 – 61.1) ^{b, c}
1-C Metabolism			
5-mTHF	6.9 (5.3 – 12.9)	6.0 (3.1 – 9.0)	ND
AMP	20.0 (9.9 – 35.1)	18.7 (10.9 – 27.5)	11.2 (4.9 – 13.7) ^{b, c}
Betaine	26.8.8 (17.1 – 35.7)	31.1 (17.9 – 32.4)	21.3 (12.6 – 25.9) ^{b, c}
Choline	117.5 (92.7 – 148.6)	122.7 (105.2 – 132.7)	116.3 (54.3 – 171.3)
Cystathionine	0.81 (0.59 – 1.12)	0.94 (0.72 – 1.17)	0.14 (0.08 – 0.19) ^{b, c}
Cysteine	2780.6 (1644.2 – 4776.9)	2528.9 (420.8 – 3746.7)	ND
Dimethylglycine	120.8 (88.9 – 146.7)	138.7 (112.6 – 171.5)	87.2 (43.6 – 122.0) ^{b, c}
dUMP	0.15 (0.11 – 0.21)	0.13 (0.10 – 0.18)	ND
Folic acid	0.012 (0.007 - 0.017)	0.010 (0.005 - 0.014)	ND
Formyl-THF	0.019 (0.012 - 0.027)	0.015 (0.011 - 0.017)	ND
Glycine	481.0 (83.3 – 817.4)	154.4 (79.7 – 251.2) ^a	ND
Homocysteine	100.7 (66.3 – 180.8)	136.6 (68.9 – 307.4)	24.2 (12.2 – 45.6) ^{b, c}
Methionine	36.2 (24.6 – 67.1)	28.7 (19.9 – 33.3) ^a	7.23 (4.9 – 10.7) ^{b, c}
NADPH	25.8 (17.9 – 32.8)	21.3 (14.1 – 26.3) ^a	7.2 (4.9 – 8.2) ^{b, c}
Pyridoxal-5-P	0.21 (0.14 – 0.28)	0.25 (0.15 – 0.38)	0.18 (0.14 – 0.28)
Riboflavin	0.34 (0.22 – 0.53)	0.33 (0.25 – 0.41)	0.22 (0.13 – 0.34) ^{b, c}
SAH	12.7 (10.7 – 15.0)	9.0 (7.6 – 10.5) ^a	2.9 (1.6 – 3.7) ^{b, c}
SAM	4.6 (2.9 – 5.5)	5.0 (3.8 – 6.9)	1.5 (0.8 – 2.7) ^{b, c}
Taurine	9.3 (7.1 – 11.9)	12.8 (9.6 – 13.6) ^a	9.7 (5.1 – 16.3)

Data are shown as median (interquartile range) in nmol/g of tissue (dry weight). AMP, Adenosine 5'-monophosphate; dUMP, Deoxyuridine monophosphate; SAH, S-adenosylhomocysteine; SAM, S-adenosylmethionine; THF, Tetrahydrofolate. Significant differences in comparisons are indicated by ^anon-NASH vs NASH, ^bNon-NASH vs 12 months after surgery. ^cNASH vs one-year after surgery (at least p<0.05) by Wilcoxon rank-sum test.

Supplementary Table S3. The effect of supplementation with cell-permeable α KG analog (DMKG) in cultured cells

	Untreated (n=6)	2 Mm DMKG (n=6)	p-value
Energy Metabolism	α-ketoglutarate 0.02 (0.02 – 0.04)	0.20 (0.13 – 0.31)	0.002
	β-hydroxybutyrate 0.27 (0.19 – 0.36)	0.33 (0.27 – 0.52)	0.240
	Alanine 1.1 (0.89 – 1.5)	4.44 (3.36 – 7.66)	0.002
	Aspartate 1.78 (1.27 – 5.14)	8.6 (5.73 – 14.45)	0.026
	(Iso)Citrate 0.16 (0.14 – 0.23)	0.29 (0.24 – 0.44)	0.041
	Fructose-1,6BP 0.91 (0.67 – 1.45)	1.51 (0.85 – 2.5)	0.240
	Fructose-6P 5.7 (3.58 – 7.51)	8.2 (5.0 – 11.9)	0.240
	Fumarate 0.13 (0.10 – 0.19)	0.6 (0.4 – 0.9)	0.002
	Glucose 10.3 (7.7 – 16.7)	8.6 (6.2 – 10.6)	0.310
	Gluconate-6P 0.23 (0.21 – 0.36)	0.34 (0.24 – 0.41)	0.485
	Glucose-6P 1.7 (1.1 – 2.6)	2.6 (1.4 – 4.2)	0.240
	Glutamate 3.0 (0.8 – 6.4)	23.9 (16.9 – 38.9)	0.002
	Glycerate-3P 1.9 (1.1 – 3.0)	4.0 (2.2 – 6.7)	0.065
	Isoleucine 1.5 (1.3 – 2.6)	1.6 (1.6 – 1.6)	0.485
	Lactate 29.5 (24.2 – 36.2)	32.6 (24.2 – 40.9)	0.818
	Leucine 3.7 (3.2 – 4.9)	4.5 (3.3 – 5.2)	0.699
	Malate 0.28 (0.25 – 0.38)	1.15 (0.86 – 1.97)	0.002
	Oxaloacetate 0.8 (0.6 – 1.2)	1.7 (1.0 – 2.3)	0.041
	Phosphoenolpyruvate 0.19 (0.08 – 0.42)	0.36 (0.24 – 0.81)	0.240
	Pyruvate 0.14 (0.11 – 0.22)	0.28 (0.22 – 0.34)	0.041
	Ribose-5P 0.26 (0.14 – 0.39)	0.40 (0.3 – 0.5)	0.132
	Serine 2.0 (1.0 – 3.1)	8.1 (5.3 – 11.7)	0.004
	Succinate 4.6 (4.5 – 5.6)	5.4 (4.2 – 7.5)	0.485
	Valine 4.5 (3.8 – 5.3)	4.8 (3.6 – 6.0)	0.818
1-C Metabolism	AMP 0.54 (0.11 – 0.67)	0.07 (0.0 5- 0.12)	0.004
	Betaine* 0.008 (0.005 – 0.010)	0.003 (0.002 – 0.005)	0.026
	Choline-Dimethylglycine 0.05 (0.03 – 0.08)	0.02 (0.01 – 0.03)	0.015
	Cystathionine* 1.9 (1.8 – 3.5)	1.8 (1.5 – 1.8)	0.015
	Cysteine 783.3 (579.1 – 1141.8)	651.6 (635.6 – 704.3)	0.485
	Folic acid* 0.42 (0.29 – 0.54)	0.24 (0.20 – 0.40)	0.180
	Formyl-THF* 0.28 (0.24 – 0.64)	0.26 (0.11 – 0.63)	0.589
	Glycine 7.1 (5.3 – 7.5)	5.7 (4.8 – 7.9)	0.699
	Homocysteine 0.011 (0.008 – 0.014)	0.007 (0.004-0.009)	0.041
	Methyl-THF* 0.50 (0.30 – 0.096)	0.33 (0.22 – 0.35)	0.093
	Methylcobalamin * 0.11 (0.06 – 0.23)	0.17 (0.15 – 0.20)	0.485
	Methionine 0.036 (0.025 – 0.076)	0.038 (0.026 – 0.068)	0.485
	NADPH 0.11 (0.08 – 0.12)	0.05 (0.03 – 0.06)	0.015
	Pyridoxal 5-P * 3.5 (3.2 – 4.9)	2.9 (2.2 – 4.6)	0.240
	Riboflavin * 0.35 (0.34 – 0.75)	0.6 (0.4 – 0.6)	0.589
	SAH* 0.010 (0.006 – 0.023)	0.008 (0.004 – 0.009)	0.009
	SAM 0.071 (0.065 – 0.080)	0.058 (0.048 – 0.065)	0.041

Data are shown as median (interquartile range) in nmol/mg of protein except those marked with an asterisk denoting pmol/mg of protein. AMP, adenosyl monophosphate; NADPH, Nicotinamide adenine dinucleotide phosphate; SAH, S-adenosylhomocysteine; SAM, S-adenosylmethionine; THF, Tetrahydrofolate.

Supplementary Table S4. Gene expression profile in NASH livers with genes listed alphabetically according to up- and down-regulation, as compared with non- NASH livers

Upregulated

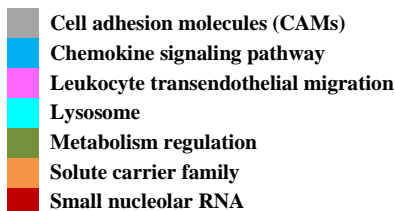
ACP5, ADCYAP1R1, AJUBA, APOL3, B3GNT5, BBC3, BHLHA15, BTG2, C12orf5, C15orf48, C2orf82, C5AR1, CAPG, CCDC109B, CCL2, CCL20, CCL3, CC, CD209, CD3G, CD52, CD83, CDCA2, CDH15, CDHR2, CFTR, CH25H, CLDN11, CLDN5, CLECL1, COL1A1, COL1A2, COL4A2-AS1, CPXM2, CPZ, CRTAM, CTSV, CXCL10, CXCL3, CXCL8, CXCL9, DOK5, DOK6, EDN2, EEF1A2, EGR2, EGR3, EZR-AS1, FABP4, FABP5, FAM151A, FAM90A7P, FAR2, Ffar3, FFAR3, FMO1, FNDC5, FOXL2, FPR2, GATA3, GEM, GLIPR1, GPNMB, GPR182, GPR183, HIST1H1B, HIST1H3B, HLA-DQA1, HLA- DRB5, HMGCS1, HSPB8, HULC, IGSF22, IL10RB-AS1, IL1B, IL4I1, INHBE, ISM1, KCNJ3, LAMP3, LINC00884, LINC00885, LOC154872, LPL, LYPD1, MB, MB21D2, MCM2, MMP9, MNDA, NANOS3, NFKBIE, NR4A3, NTN3, OSM, PADI1, PCDH9-AS2, PEG10, PLA2G7, PLAUR, PLCXD2, PLXNC1, PODN, PRAMEF10, PROK2, PSRC1, QPCT, RASSF9, RFTN1, RGS16, RGS2, RNF186, RRAD, SEC14L3, SIX1, SLC22A13, SMIM24, SORT1, SPP1, SQLE, STMN2, TACC3, TBXAS1, THBS2, THEMIS, THY1, TIFAB, TLR9, TM4SF19, TMEM200A, TNFAIP3, TNFSF9, TREM2, TRHDE-AS1, TRIM59, TRIM63, TYMS, UGT3A2, UHRF1, UNC93A, WNT2, WNT5A, ZNF620, ZNF683

Downregulated

AASS, ABCA10, ACKR2, ACOT6, ADAM1A, ADCY1, ADCY10, ADHFE1, ADTRP, AFF3, AFG3L1P, AGR2, AKR1C6P, ALPK2, ANKRD23, ANO8, ARHGEF26, ARHGEF4, C1orf228, C1QTNF3, CA3, CA9, CAPN3, CATSPER3, CCDC158, CCDC162P, CCDC180, CCDC38, CCDC84, CELSR3, CENPJ, CFAP70, CHAD, CHKB, CHRD, CIART, CIT, CLASRP, CLCN2, CMYA5, COLCA2, CPT1B, CRYGS, CSPP1, CXCL2, CYP1A1, CYP3A4, CYP3A43, CYP3A5, CYP3A7, CYP4Z1, DCDC5, DCPS, DDX43, DFNB59, DGCR14, DKFZp434J0226, EFCAB1, ENO1-AS1, ERN1, FAM132A, FAM193B, FAM76B, FAM83A-AS1, FKBP5, FLJ21408, FLJ31104, FOXO1, FUT3, GADD45G, GNMT, GNRH1, GOLGA7B, GPR128, GPT2, GSTA7P, HAL, HERC2P2, HERC2P7, HERC5, HGD1B, HORMAD2, HSD17B3, HSD3B1, ICA1, IFRD1, IGF1, IGFBP2, INS-IGF2, IRX3, ITGA10, KCNMB3, KGFLP1, KIAA0895L, KPNA7, KRT42P, KRT71, L3MBTL1, LCE2D, LGI4, LGSN, LHX4-AS1, LINC00238, LINC00659, LINC00939, LINC01125, LOC100270804, LOC100289230, LOC100505918, LOC285626, LOC644656, LOC729603, LRRC73, LYGI, MAST2, MEGF6, MREG, MT1IP, MTHFD2L, MTUS2, MYO15A, MYOM1, NBPF14, NEAT1, NEIL1, NINJ2, NNMT, NOXO1, NRBP2, OAT, P4HA1, PAPD7, PAQR6, PARP6, PATL2, PDZD3, PILRA, PILRB, POFUT2, POU6F1, PPARGC1A, PRR26, PRSS50, PSPH, PTPRH, PYROXD2, PZP, RAD51AP2, RDH12, REC8, RFPL4AL1, RHBG, RIC3, S100A1, SEC16B, SH2B1, SH2D6, SLC10A5, SLC16A1, SLC23A2, SLC25A18, SLC29A2, SLC34A1, SMIM5, SNORA33, SNORA41, SNORA6, SNORA70B, SNORA70C, SNORA70E, SN, SNORD18C, SNOR, RD98, SOCS2, S, S1R3, TAS2R19, TBC1D3B, TBC1D3C, TCAF2, TCERG1, TDRD6, TFRC, TG, TMCO6, TPTE2P5, TRPV1, TSKU, TSNAXIP1, UBE2Q2L, UCN, UGT2A1, VCPKMT, WDR60, ZDHHC11, ZNF211, ZNF266, ZNF276, ZNF507, ZNF833P

Gene ontology analysis

0



Supplementary Table S5. Gene expression data in NASH livers with up- and down-regulation, as compared with non-NASH patients.

Upregulated genes								Downregulated genes							
GeneName	log2FoldChange	p_value	GeneName	log2FoldChange	p_value	GeneName	log2FoldChange	p_value	GeneName	log2FoldChange	p_value	GeneName	log2FoldChange	p_value	
LINC00885	1.108266051	0.002829371	CAPG	1.3101614	0.00197551	WDR60	-1.126493661	0.001774784	PTPRH	-1.11299621	0.001893405	POU6F1	-1.85739276	0.000468	
TNFSF9	1.605596145	0.001640699	LAMP3	1.03442289	0.01288156	GADD45G	-1.947612699	0.005103815	CA9	-1.14424059	0.026604041	ARHGEF26	-1.20780671	0.009858	
RNF186	1.536754651	0.042777861	FMO1	1.88537491	0.00909886	IGFBP2	-2.142189864	0.004480224	RRR26	-1.16557451	0.014913984	ADCY10	-2.0612402	0.005347	
IL10RB-A51	1.135618936	0.002732591	GEM	2.12676185	0.01258329	CRYGS	-1.368207074	0.036291373	KPNA7	-1.14681521	2.33E-05	ABCAL10	-1.17408381	0.035637	
BHLHA15	1.119858021	0.01377422	CXCL9	1.03320944	0.00727778	PILRA	-1.323211487	0.016119236	NOXO1	-1.44398216	0.000494939	ICAI1	-1.34728989	0.00753	
ZNF683	1.161298268	0.001273694	RAR2	1.09681995	0.01731577	CHAD	-1.079216635	0.008185086	EFCAB1	-1.24525592	0.003888249	CAPN3	-1.75328208	0.012313	
PPR2	1.445569009	0.008564473	MMP9	1.47015816	0.000163	ARHGEF4	-1.49195251	0.004623492	LOC100289230	-1.31613538	0.024469741	SYBU	-1.24599129	0.00974	
HIST1H1B	1.251730534	0.040270009	PLA2G7	1.43160207	0.00188927	DKFZp434J0226	-1.217881339	0.047275558	PAPPD	-1.13453724	0.025046828	DDX43	-1.55364884	0.00163	
FOXL2	1.145449548	0.04465113	RGS16	1.45828142	0.03771505	CYP3A5	-2.00176286	0.007499079	TCERG1	-1.05862387	0.003162446	SNORA41	-1.35308048	0.019492	
SEC14L3	1.207605709	0.00668581	LYPD1	1.08815201	0.02034367	SEC16B	-1.060531976	0.003476521	NNMT	-1.4945219	0.004529442	MTUS2	-1.37975481	0.035259	
IGSF22	1.494253964	0.027197341	CDH15	1.39545464	0.03108971	ACOT6	-1.054823819	0.009864916	CHRD	-1.79152394	0.027862136	SNTF276	-1.52707457	0.010258	
STMN2	2.188089325	0.00933607	CCNB2	1.06475296	0.04162568	CLCN2	-1.28755502	0.00532075	ADTRP	-1.01349889	0.00129832	PATL2	-1.0902415	0.025103	
GPR183	1.271443475	0.000440736	EEF1A2	1.89120342	0.00648014	KRT71	-1.340791372	0.002811005	LGSN	-1.0940202	0.002486112	HERC2P2	-1.35457536	0.031157	
CCL2	1.634426073	0.043998043	FCAMR	1.53439159	0.0042068	FAM19B	-1.10139395	0.013505843	TCAF2	-1.18040508	0.035311117	AASS	-1.43536492	0.009894	
RGS2	0.048396224	0.006946685	IL1B	1.94459522	0.0027467	GPT2	-1.273625123	0.00983449	FAM76B	-1.32957049	0.011563721	CA3	-1.12532466	0.006789	
EDN2	1.4333565	0.015961887	FAM151A	1.44265347	0.02711086	IGF1	-1.110791211	0.006389929	TBC1D3B	-1.7122397	0.035138425	MT1P	-1.57448536	0.045721	
SPP1	1.214260744	0.028256747	GPMMB	1.1812359	0.02641774	CYP3A7	-1.943510904	6.42E-05	PILRB	-1.71640567	0.04625982	AN08	-1.20068677	0.00444	
NR4A3	1.375631513	0.032454529	IL4I1	1.11818242	0.00628265	CIT	-1.240458536	0.001098771	LOC100270804	-1.472921668	0.001714085	SNORA33	-1.22208689	0.017547	
FABP5	1.497196087	0.001625692	ADCYAP1R	1.02506482	0.02922941	LYG1	-1.586894371	0.023798416	AGR2	-1.7968788	0.037994226	ZNF507	-1.43590952	0.020977	
HIST1H3B	1.206176166	0.002622831	MB21D2	1.07487323	0.02649904	HERC2P7	-1.174357222	0.029563383	NRBP2	-1.031481993	0.006090631	SNORA70E	-1.14289444	0.041911	
CLEC1L	1.238343858	0.045646541	NTN3	1.00953129	0.01187354	VCPKMT	-1.010084239	0.005192634	CCDC180	-1.61698831	0.024718146	RHBG	-1.44976652	0.014181	
COL1A2	1.140998788	0.001725005	EGR3	1.73474765	0.03692354	CATSPER3	-1.181362923	0.005549189	SLC23A2	-1.01411492	0.041434011	MEGF6	-1.01968955	0.027641	
CPZ	1.057332448	0.037351842	UNC93A	1.0991426	0.01985908	UCN	-1.042298141	0.049830757	SLC34A1	-1.34181598	0.016120516	PARGC1A	-1.0547058	0.043285	
OSM	1.57816567	0.000431245	BTG2	1.3793159	0.01114981	CCDC162P	-1.361185035	0.004456451	SMIM5	-1.02437494	0.02913347	MTHFD2L	-1.35439167	0.004165	
CCL3	1.114250666	0.024238018	CDCA2	1.00829354	0.02227709	LRRK73	-1.328380079	0.009472993	TRPV1	-1.38803877	0.030937051	CENPJ	-1.02879915	0.030369	
WNT2	1.129255588	0.046624632	QCT	1.15605831	0.00822221	LOC100505918	-1.618054831	0.000383718	AFF3	-1.1349031	0.013133814	SNORD18C	-1.52765816	0.035507	
GATA3	1.225255948	0.007728114	AUBA	1.12998723	0.04753186	ZDHHC11	-1.470278778	0.003716059	PAQR6	-1.23357586	0.034895557	CELSR3	-1.36441169	0.00912	
PADI1	3.066689154	0.002092239	EZR-AS1	1.4489299	0.0317027	KRT42P	-1.569628795	0.0109052349	CSPP1	-1.03610211	0.008362508	SLC16A1	-1.06181711	0.016263	
CLDN5	1.021312659	0.033108993	COL1A1	1.21886276	0.0267172	S100A1	-1.013531104	0.005872988	ZNF266	-1.02918135	0.003050812	C1orf228	-1.67870492	0.02814	
SIX1	1.240592269	0.014864258	APOL3	1.0782398	0.00497664	RIC3	-1.39931336	0.001679726	TDRD6	-1.4872688	0.039793123	NEIL1	-1.05645288	0.015188	
THEMIS	1.005995323	0.000895744	PSRC1	1.06741263	0.04120535	DFNB59	-1.609085539	0.001677429	PRSS50	-1.47990009	0.011927551	SH2D26	-1.36150159	0.018901	
HSPB8	1.177115944	0.018070953	RASSF9	1.08026457	0.03333617	LINCO0659	-1.194626299	0.00017105	CXCL2	-1.39777064	0.033398815	TSKU	-1.05789448	0.000901	
LPL	2.481562055	0.001204697	ACP5	1.013975591	0.02173683	UBE2Q2L	-1.084875159	0.032211551	SHB2B1	-1.007071018	0.010187832	CYP4Z1	-1.6292643	0.005059	
CXCL3	1.085612193	0.046317488	FAM90A7P	1.43185238	0.03039275	ADCY1	-1.035330066	0.009044822	CMYA5	-1.88961818	0.004205976	ITGA10	-1.85265283	0.007251	
TRHDE-AS1	1.432880463	0.001455994	PODN	1.39243877	0.01026783	TSNAXIP1	-1.244770891	0.007667743	P4HA1	-1.72685563	0.000608092	C1QTNF3	-1.1330806	0.020593	
CCL20	1.619794764	0.033642148	TRIM59	1.0333655	0.00549998	NEAT1	-2.100398711	0.023090165	HSD17B8	-1.26045501	0.049483051	OAT	-1.30476489	0.015518	
LINCO0884	1.008899566	0.030495083	CDHR2	1.25087376	0.00502943	SNORA72	-1.274518492	0.022261622	FLJ21408	-1.70077327	0.025709691	KIAA0895L	-1.65475067	0.047397	
DOK5	1.321334784	0.031174145	MB	1.84880994	0.00665582	FKBP5	-1.425452759	0.047662255	RPL41AL1	-1.18552877	0.046163437	AFG31L1P	-1.33548026	0.045384	
CLDN11	1.016851801	0.011762836	SMM24	2.30730749	0.01916011	ZNF211	-1.251199378	0.016830068	CIART	-1.15097359	0.047524274	CYP1A1	-1.75334242	0.011345	
CD3G	1.084529628	0.0236164364	TLR9	1.10858318	0.02735103	GOLG7A8	-1.17791694	0.028403328	LINC01125	-1.44058468	0.034571851	HAL	-1.57754608	0.020219	
MNDA	1.034074048	0.016435588	INHBE	1.13739729	0.01880832	CCDC84	-1.15751599	0.018016694	SOCS2	-1.71615046	0.000992992	GNMT	-1.16873572	0.015956	
UHFR1	1.314983104	0.002832784	COL4A2-AS1	1.25129413	0.03020565	GNRH1	-1.007087074	0.021117891	FAM132A	-1.16590025	0.029318286	SNORA70C	-1.49826649	0.029462	
CD52	1.399552461	1.89E-05	B3GNT5	1.2871771	0.01160255	ADHFE1	-1.129910777	8.13-E05	KCNMB3	-1.33571172	0.032448127	SLC10AS	-1.29351273	0.002953	
HLA-DQA1	1.74762449	0.02459273	BBC3	1.07223164	0.00516045	TAS1R3	-1.204752139	0.026564907	LOC644656	-1.265457533	0.036935159	KGFLP1	-1.11942506	0.027451	
LOC154872	1.313600864	0.005456459	PRAME10	2.04642563	0.00228353	LINCO0238	-1.352417355	0.000206214	PARP6	-1.00612529	0.038261869	SLC25A18	-1.67830532	0.018477	
CTSV	1.16256244	0.002183877	TMEM159	1.28956999	0.00844104	TG	-1.362292804	0.001615655	ERN1	-1.15768826	0.025821033	ALPK2	-1.03852867	0.004912	
HMGCS1	1.13009153	0.001204527	CD83	1.70461926	0.0080599	UGT2A1	-1.6555474606	0.047696138	TAS2R19	-1.51169392	0.004660052	LOC79603	-1.23185661	0.011661	
NANOS3	1.252378255	0.000139541	PLXNC1	1.31395716	0.01916546	SLC29A2	-1.006325302	0.003901491	HERC5	-1.00498747	0.000740968	REC8	-1.11254282	0.030743	
GLIPR1	1.036426354	0.010689844	FFAR3	1.5142500	0.00897662	CCDC158	-1.456799089	0.020690154	FLJ31104	-1.17486704	0.007729886	CYP3A43	-2.31859675	0.002867	
THB52	1.032338806	0.003884552	WNT5A	1.07413561	0.01195956	CPT1B	-1.670810078	0.0436173	DCPS	-1.26871742	0.019435557	PSPH	-1.87290395	0.012305	
FNDC5	1.406618425	0.019345272	CCDC109B	1.13499699	0.00448924	LINCO00939	-1.55396493	0.014501206	EN01-A51	-1.45557871	0.005486	EN01-A51	-1.45557871	0.005486	
TIFAB	1.523492563	0.00809768	PEG10	2.48542661	0.0069961	MAST2	-1.125526239	0.016840142	DCDC5	-1.77184007	0.004577131	ACKR2	-1.09748842	0.017915	
C2orf82	1.170991787	0.001451408	PLUR	1.5661879	0.001565	GSTA7P	-1.714817218	2.46-E-05	HSD3B1	-1.1444667	0.014152964	RDH12	-2.07750891	0.00122	
SORT1	1.023260495	0.015972087	PLCXD2	1.34094042	0.02312495	LHX4-A51	-1.371608943	0.0325							

Supplementary Table S6. List of altered CpG sites in NASH livers, as compared with non- NASH livers

Gene Name	CpG	Gene Name	CpG	Gene Name	CpG	Gene Name	CpG	Gene Name	CpG
A2ML1	cg12168926	C1orf54	cg06334965	CYP2C19	cg24857560	FGD4	cg11809958	HMOX2	cg02873098
ABCC3	cg18891141	C20orf78	cg19205181	CYP7A1	cg15805923	FGFR1	cg23518439	HNF4A	cg23834593
ACP5	cg01524690	C2orf54	cg20140201	DCC	cg02835371	FKBP5	cg21517946	HNRPKP3	cg01405920
ACTN1	cg04425263	C5orf56	cg03168315	DEFB119	cg13817555	FKBP5	cg21517946	IDH3B	cg27161589
ADAMDEC1	cg18212777	C5orf66	cg25768573	DEFB121	cg13795252	FKBP5	cg21517946	IGF2	cg08686462
ADAMTS14	cg26971530	CAD	cg25258016	DEFB126	cg01745599	FGF22	cg23518439	IGSF8	cg12390003
ADAMTS16	cg07834743	CARD10	cg16026346	DEFB132	cg08841021	FGFR1	cg15791248	IKZF1	cg01139861
ADIG	cg13816419	CCDC122	cg13487505	DHRS7B	cg19360316	FKBP5	cg21517946	IL32	cg20877076
AKR1C4	cg06573570	CCDC129	cg23825123	DHRS7B	cg05694098	FLG	cg19855573	IPCEF1	cg19690214
AMPH	cg14920977	CCDC144NL	cg22570042	DISP2	cg17063840	FOXI1	cg07849278	ISM1	cg15577927
ANKRD34C-AS1	cg15981071	CCDC15	cg20250779	DLGAP1	cg25358264	FOXO1	cg02202169	ITGA4	cg25515269
ANKS1B	cg18299299	CCDC166	cg08435853	DNAAF3	cg09204255	FYN	cg08061598	IYD	cg08400967
APH1B	cg09264088	CCDC166	cg14540594	DOC2A	cg19699287	GABARAP	cg16879549	KCNAA3	cg00995520
APOBEC2	cg09841052	CCDC59	cg03652173	DOCK10	cg19407684	GALNT1	cg16741573	KCNK10	cg01523348
ARHGEF4	cg09015973	CCT8L2	cg02601618	DPYSL3	cg13669166	GAPDH	cg15729137	KCNQ1	cg23623667
ARL4A	cg07227033	CDC23	cg24961402	DUSP1	cg06819445	GATM	cg11032707	KDMSB	cg08718872
ARL8A	cg08649954	CEACAM21	cg04946843	ECHDC2	cg06600287	GBA3	cg17751101	KIAA0319	cg18433519
ARPP21	cg10504927	CH13L1	cg14085262	EEF1D	cg14824382	GGAA2	cg05579124	KIAA0319	cg12349317
ARSK	cg11569235	CHMP6	cg00774579	EFHD1	cg17021917	GGPS1	cg10107779	KIAA0319	cg00944873
ATCAY	cg08000406	CHST8	cg24221853	EIF2AK2	cg23820429	GPLD1	cg02346062	KIAA0319	cg16906346
ATG101	cg18315870	CHST9	cg01960885	EIF4ENIF1	cg01782953	GPR160	cg14168775	KIAA1191	cg26620356
ATG101	cg05628902	CLDN18	cg20366986	ELAC1	cg20726616	GPR75	cg20081082	KIF14	cg22888029
ATP5A1	cg26626598	CLEC1B	cg27583026	ELAVL4	cg25217583	GPS2	cg12391328	KLB	cg06321636
ATP6V0E2	cg18934443	CLEC3B	cg22505962	ELAVL4	cg09784523	GRAMD3	cg06609646	KLF5	cg20314763
ATP6V1G1	cg14391907	CLIC3	cg23224755	ELF1	cg15040708	GSDMB	cg10057218	KLK8	cg13388253
BATF	cg21158815	CLVS2	cg20134787	ELOVL3	cg24362923	GSX1	cg10071824	LDHAL6A	cg0688460
BCAT1	cg20783223	CMTM3	cg12370353	ENPP3	cg12121052	GTF2A2	cg00368989	LGALS8	cg0427302
BCL7A	cg10552903	CNBP	cg02658946	ESR1	cg02583095	GTF2IRD1	cg07645228	LILRA2	cg23089880
BCL7C	cg13914857	CNGA3	cg00209520	ETNK1	cg21477262	GULP1	cg08913189	LIMK2	cg01606027
BCL9L	cg20029201	CNNM1	cg06312469	EXPH5	cg14140118	GZMA	cg13566919	LINCO1146	cg24014326
BDNF	cg06260077	CNTN1	cg24360230	FABP12	cg18190353	H19	cg06658831	LINCO1168	cg15681295
BIN1	cg02161262	COLEC12	cg21067023	FAIM3	cg17460386	HAO1	cg01478327	LOC441666	cg24527560
BOLL	cg10547527	COXA72	cg25716013	FAM118A	cg00733150	HARS2	cg26273129	LPPIR1	cg04778212
BOLL	cg06077337	CR1	cg25029035	FAM193B	cg18478850	HAS3	cg09944073	LRRC10B	cg06964190
BRCA1	cg14947218	CRYBG3	cg22429199	FAM222A	cg14544673	HCST	cg16001418	LRRC55	cg03717588
BRCA1	cg02286533	CRYZL1	cg16762072	FAM60A	cg01611280	HDAC9	cg19585556	LRRTM1	cg26157270
C17orf98	cg18343108	CTSV	cg24546976	FBXO34	cg18427465	HIBCH	cg06484496	LRRTM3	cg09455274
C17orf98	cg12552293	CYB5R3	cg18535283	FCRLA	cg05033369	HIST1H2BE	cg22942804	LSP1	cg15348841
C19orf84	cg11030887	CYP2C19	cg27505447	FERMT1	cg25325723	HLF	cg25534244	LTBR	cg10452531
Gene Name	CpG	Gene Name	CpG	Gene Name	CpG	Gene Name	CpG	Gene Name	CpG
MAD2L1	cg14360823	OR7D4	cg04487907	RGS14	cg15591490	SPSB2	cg09080114	VMO1	cg24874612
MAGOHB	cg03208983	OSMR	cg19609242	RGS14	cg11370586	ST3GAL1	cg02637438	VPS39	cg14774557
MAL2	cg02085119	P2RX6	cg09854409	RGS4	cg20056654	ST6GALNAC2	cg21914725	WBP2NL	cg08431931
MANSC4	cg13312247	P2RX7	cg08688169	RGS5	cg17683793	ST6GALNAC4	cg13886636	WBP2NL	cg04717802
MARK3	cg26623547	PAK1IIP1	cg12409563	RIBC2	cg18180155	STMN2	cg13068285	WBP2NL	cg25099233
MARS	cg06714758	PCDH2A	cg27546766	RIBC2	cg05742863	STT3A	cg19571034	WISP1	cg13358979
MBIP	cg12645564	PCDH8	cg02326566	RIBC2	cg00610021	SUSD5	cg03497399	WNT3	cg11142826
MED9	cg00723891	PCDHB12	cg17101542	RNF14	cg21256257	SYNJ1	cg18548246	WNT9A	cg05183226
MFAP1	cg12801082	PCDHB12	cg15548198	RNF214	cg04174309	TAB2	cg06416086	YAPI	cg12697442
MGAT4A	cg14223723	PCDHB2	cg23969338	RNF25	cg26548497	TAGLN	cg11861562	ZBTB48	cg19508900
MGC2782	cg13296396	PCDHGB4	cg22648135	RNP51	cg08301299	TARSL2	cg10526733	ZCCHC4	cg13975540
MICAL3	cg06200397	PCP2	cg03489492	RORB	cg14503744	TBC1D1	cg06331663	ZFR2	cg08098382
MOBP	cg27272723	PDE4B	cg10277218	RPA3	cg26322315	TDRD6	cg08426066	ZNF197	cg11557071
MORF4L1	cg20596706	PDE4D	cg04545873	RPS6KL1	cg12643970	TDRD6	cg11931223	ZNF260	cg24909706
MRPL34	cg01445659	PEX2	cg22944540	RSPH6A	cg02505812	THAP1	cg20173334	ZNF287	cg12597066
MRPS10	cg24613956	PIAS3	cg15978276	RSPH6A	cg07377422	TMC01	cg10234330	ZNF474	cg18554917
MTAP	cg23850567	PKIA	cg04689061	SAMD3	cg09345868	TMEM105	cg21591452	ZNF527	cg19000959
MVB12A	cg02608002	PLCD4	cg18771537	SCARNA6	cg24516399	TMEM105	cg06727703	ZNF883	cg02199333
MYOIC	cg12741184	PLIN1	cg08749443	SCML4	cg08792995	TMEM132E	cg21745612	ZP2	cg18249108
MYOCD	cg18181954	POTEA	cg01192262	SEC11C	cg20600053	TMEM194A	cg01217666		
NCCR1	cg18627816	PPBP	cg20543211	SENP1	cg12381317	TMEM200B	cg15307678		
NDUFAF3	cg07109801	PPM1A	cg14785542	SETD9	cg06961054	TMEM200B	cg22788029		
NDUFB10	cg07623113	PSG6	cg20120646	SETD9	cg06795995	TMEM217	cg18131329		
NKK6-2	cg17996619	PTCHD3	cg09544380	SHD	cg24830664	TMEM217	cg00480799		
NLRP6	cg09205751	PTH2	cg22250242	SHPK	cg21817720	TNFAIP8L2	cg22392857		
NOSIP	cg06468619	PTPN7	cg01520554	SIRT6	cg05075545	TRAPPC1	cg10518440		
NRON	cg09518226	PWWP2A	cg20433356	SLC10A5	cg20769419	TRIM7	cg16027343		
NUDT21	cg14837652	PYCARD	cg09115984	SLC15A5	cg26345444	TRIM8	cg00793774		
OLFM3	cg16510022	RAB1B	cg25618573	SLC29A2	cg07183539	TRIP10	cg18732869		
OLFML2A	cg25612362	RAB1B	cg04592747	SLC6A4	cg06841846	TRIT1	cg04921771		
OR14I1	cg25289056	RAB1B	cg15201417	SLC7A8	cg21380590	TRPC6	cg07898145		
OR1A2	cg03271520	RAB31	cg04995377	SMG6	cg27337217	TSACC	cg19759212		
OR2L8	cg16077391	RAB37	cg08080145	SNCB	cg25444839	TWIST1	cg14391419		
OR2L8	cg18857759	RALGAPB	cg15971382	SND1	cg04345581	TXNL1	cg00152799		
OR4D1	cg12463722	RANBP3	cg08371934	SND1	cg11539674	TYW3	cg12981534		
OR4D1	cg20221991	RAPGEF1	cg15815515	SNORA71C	cg11363483	UCHL3	cg07830652		
OR4D2	cg24269480	RASSF5	cg16122716	SNX13	cg06049192	UGT3A2	cg10402936		
OR51B2	cg12036731	RBKS	cg16651262	SPDYC	cg03196265	UTS2	cg15727920		
OR51Q1	cg05975928	RET	cg01289552	SPRR2C	cg07804289	VIL1	cg18970338		

Supplementary Table S7. List of antibodies and dilutions used in immunoblot analyses

Antigen	Primary Antibody	Dilution	Secondary Antibody	Dilution
4-HNE	4-HNE antibody, #393206 (Millipore)	1:1000	Goat α-rabbit HRP, P0448 (Dako Agilent, Santa Clara CA)	1:5000
Actin	Pan-Actin antibody, #4968 (Cell signalling, Danvers, MA)	1:10000	Goat α-mouse, HRP, 1D3 (Dako Agilent, Santa Clara CA)	1:5000
AMPK-pT172	pAMPK Antibody, #2531 (Cell signalling, Danvers, MA)	1:1000	Goat α-rabbit HRP, P0448 (Dako Agilent Santa Clara CA)	1:5000
AMPK	AMPK Antibody #2532S (Cell signalling, Danvers, MA)	1:1000	Goat α-rabbit HRP, P0448 (Dako Agilent, Santa Clara CA)	1:5000
AKT-pT308	p-Akt Antibody, #4056 (Cell signalling, Danvers, MA)	1:1000	Goat α-rabbit HRP, P0448 (Dako Agilent, Santa Clara CA)	1:5000
AKT-pT473	p-Akt Antibody, #4060 (Cell signalling, Danvers, MA)	1:1000	Goat α-rabbit HRP, P0448 (Dako Agilent, Santa Clara CA)	1:5000
AKT	AKT Antibody, #4685 (Cell signalling, Danvers, MA)	1:1000	Goat α-rabbit HRP, P0448 (Dako Agilent, Santa Clara CA)	1:5000
ATG5	ATG7 Antibody, #12994 (Cell signalling, Danvers, MA)	1:1000	Goat α-rabbit HRP, P0448 (Dako Agilent, Santa Clara CA)	1:5000
mTOR-pS2448	p-mTOR Antibody, #2971 (Cell signalling, Danvers, MA)	1:1000	Goat α-rabbit HRP, P0448 (Dako Agilent, Santa Clara CA)	1:2000
mTOR	mTOR Antibody, #2972 (Cell signalling, Danvers, MA)	1:200	Goat α-rabbit HRP, P0448 (Dako Agilent, Santa Clara CA)	1:2000
S6-pS235/236	p-S6 Antibody, #4856 (Cell signalling, Danvers, MA)	1:1000	Goat α-rabbit HRP, P0448 (Dako Agilent, Santa Clara CA)	1:5000
S6	S6 Antibody, #2217 (Cell signalling, Danvers, MA)	1:1000	Goat α-rabbit HRP, P0448 (Dako Agilent, Santa Clara CA)	1:5000
S6K-pS235/236	p-S6K Antibody, #9205 (Cell signalling, Danvers, MA)	1:1000	Goat α-rabbit HRP, P0448 (Dako Agilent, Santa Clara CA)	1:5000
S6K	S6K Antibody, #2708 (Cell signalling, Danvers, MA)	1:1000	Goat α-rabbit HRP, P0448 (Dako Agilent, Santa Clara CA)	1:5000
BAX	BAX Antibody, #5023 (Cell signalling, Danvers, MA)	1:1000	Goat α-rabbit HRP, P0448 (Dako Agilent, Santa Clara CA)	1:5000
4EBP1-pT37/46	p-4E-BP1 Antibody, #2855 (Cell signalling, Danvers, MA)	1:1000	Goat α-rabbit HRP, P0448 (Dako Agilent, Santa Clara CA)	1:5000
p62/SQSTM1	SQSTM1 / p62 Antibody, #5114 (Cell signalling, Danvers, MA)	1:1000	Goat α-rabbit HRP, P0448 (Dako Agilent, Santa Clara CA)	1:5000
Caspase 3	Cleaved Caspase-3 Antibody, #9664 (Cell signalling, Danvers, MA)	1:1000	Goat α-rabbit HRP, P0448 (Dako Agilent, Santa Clara CA)	1:5000
Caspase 8	Caspase-8 Antibody, #9746 (Cell signalling, Danvers, MA)	1:1000	Goat α-rabbit HRP, P0448 (Dako Agilent, Santa Clara CA)	1:5000
Caspase 9	Caspase-9 Antibody, C7729 (Sigma, Saint Louis, MO)	1:1000	Goat α-rabbit HRP, P0448 (Dako Agilent, Santa Clara CA)	1:5000
SAPK/Jnk-p	SAPK/JNK-p Antibody, #9251 (Cell signalling, Danvers, MA)	1:1000	Goat α-rabbit HRP, P0448 (Dako Agilent, Santa Clara CA)	1:5000
MAK (Erk1/2) p-P44/42	p-P44/42 ERK1/2 Antibody, #9101 (Cell signalling, Danvers, MA)	1:1000	Goat α-rabbit HRP, P0448 (Dako Agilent, Santa Clara CA)	1:5000
MAPK (Erk1/2) P44/42	P44/42 ERK1/2 Antibody, #9102 (Cell signalling, Danvers, MA)	1:1000	Goat α-rabbit HRP, P0448 (Dako Agilent, Santa Clara CA)	1:5000
IL10	IL10 antibody, ab34843 (Abcam, Cambridge, UK)	1:1000	Goat α-rabbit HRP, P0448 (Dako Agilent, Santa Clara CA)	1:5000
MFN2	MFN2 Antibody, ab127773 (Abcam)	1:1000	Goat α-rabbit HRP, P0448 (Dako Agilent, Santa Clara CA)	1:5000

NFKB	NFKB p65 Antibody, #8242 (Cell signalling, Danvers, MA)	1:1000	Goat α -rabbit HRP, P0448 (Dako Agilent, Santa Clara CA)	1:5000
OXPHOS	OXPHOS Antibody, ab110411 (Abcam)	1:250	Goat α -mouse, HRP, 1D3 (Dako Agilent, Santa Clara CA)	1:5000
p38	p-p38 MAPK Antibody, #9211 (Cell signalling, Danvers, MA)	1:1000	Goat α -rabbit HRP, P0448 (Dako Agilent, Santa Clara CA)	1:5000
STAT3-pT705	p-STAT3 Antibody, #9145 (Cell signalling, Danvers, MA)	1:1000	Goat α -rabbit HRP, P0448 (Dako Agilent, Santa Clara CA)	1:5000
STAT3	STAT3 Antibody, #9139 (Cell signalling, Danvers, MA)	1:1000	Goat α -mouse HRP, P0447 (Dako, Agilent, Santa Clara CA, USA)	1:5000
LC3B	LC3B Antibody, #2775S (Cell signalling, Danvers, MA)	1:1000	Goat α -rabbit HRP, P0448 (Dako Agilent, Santa Clara CA)	1:5000
LAMP2A	LAMP2A Antibody, ab125068 (Abcam)	1:1000	Goat α -rabbit HRP, P0448 (Dako Agilent, Santa Clara CA)	1:5000
FASN	FASN Antibody, #3180 (Cell signalling, Danvers, MA)	1:1000	Goat α -rabbit HRP, P0448 (Dako Agilent, Santa Clara CA)	1:5000
TOM20	Tom20 Antibody, #42406 (Cell signalling, Danvers, MA)	1:1000	Goat α -rabbit HRP, P0448 (Dako Agilent, Santa Clara CA)	1:5000
MFN2	MFN2 Antibody, ab127773 (Abcam)	1:1000	Goat α -rabbit HRP, P0448 (Dako Agilent, Santa Clara CA)	1:5000
FAH	FAH Antibody, #ABN526 (Millipore, Massachusetts, MA)	1:1000	Goat α -rabbit HRP, P0448 (Dako Agilent, Santa Clara CA)	1:5000
GADPH	GADPH Antibody, #2118 (Cell signalling, Danvers, MA)	1:8000	Goat α -rabbit HRP, P0448 (Dako Agilent, Santa Clara CA)	1:5000

Supplementary Table S8. List of reagents and procedures provided via Taqman® gene expression assays used in quantitative RT-PCR. The expressions of housekeeping gene 18S (Hs03928985_g1) were used for calculations

Gene expression assay	Gene name
aKGDH Hs01081865_m1	Alpha-Ketoglutarate Dehydrogenase
ACACA Hs01046047_m1	Acetyl-CoA Carboxylase Alpha
ACLY Hs00153764_m1	ATP citrate lyase
IDH1 Hs00271858_m1	Isocitrate Dehydrogenase 1
IDH2 Hs00953881_m1	Isocitrate Dehydrogenase 2
IDH3A Hs00194253_m1	Isocitrate Dehydrogenase 3A
GSL1 Hs00248163_m1	Glutaminase
GLUD1 Hs03989560_s1	Glutamate Dehydrogenase 1
PC Hs00559398_m1	Pyruvate Carboxylase
SDHB Hs01042482_m1	Succinate Dehydrogenase B
ACP5 Hs00356261_m1	Acid Phosphatase 5, Tartrate Resistant
ARL8A Hs00373395_m1	ADP Ribosylation Factor Like GTPase 8A
C1orf54 Hs04398113_m1	Chromosome 1 Open Reading Frame 54
DISP2 Hs00394338_m1	Dispatched RND Transporter Family Member 2
HDAC9 Hs00206843_m1	Histone Deacetylase 9
MARK3 Hs01058270_m1	Microtubule Affinity Regulating Kinase 3
RAB31 Hs00199313_m1	RAB31, Member RAS Oncogene Family
TDRD6 Hs01597145_m1	Tudor Domain Containing 6
TRIP10 Hs01012747_m1	Thyroid Hormone Receptor Interactor 10
UGT3A2 Hs04177793_m1	UDP Glycosyltransferase Family 3 Member A2
ZNF197 Hs01560359_m1	Zinc Finger Protein 197

Supplementary methods

Extended Study design and participants

Patients are included consecutively after previous failure in management after dietary treatments, changes in lifestyle factors and psychological assessment. We matched as closely as possible patients with and without NASH, and NASH patients agreed to have a second liver biopsy at 1 year after successful surgery. Before surgery, the drug schedule was revised and some were interrupted, especially metformin, to avoid described side effects. Some drugs were again prescribed after surgery according to the clinical follow-up. Some variables depicted in Table S8 indicated that weight loss and improvement of glucose and lipid metabolism were fully achieved during the first year. When necessary, healthy non-obese controls were used as described.¹ Clinical indication for laparoscopic sleeve gastrectomy (LSG) was according to guidelines currently used in pre-operative evaluation. We excluded patients with current, or past, history of daily alcohol abuse (≥ 30 g for men and ≥ 20 g for women), long-term consumption of hepatotoxic drugs, and liver disease of infectious origin. LSG was performed under general anaesthesia with the patient in the Lloyd-Davies position. A five-port technique was used in all patients. The greater gastric curvature was dissected, separated from the gastroepiploic arcade of the greater omentum, and continued to the His angle. The gastric transection was performed under the guidance of a 38-Fr Faucher bougie. Three cm was the distance from the pylorus to the first section point. The suture line was reinforced using polycarbonate derivatives of polyglycolic acid to avoid haemorrhages and leaks. A methylene blue leak was always performed before closing abdominal wall.^{2,3}

Transmission electron microscopy

Small pieces of the liver were first fixed in a 2% glutaraldehyde solution (pH 7.4), washed with 0.1 M cacodylate and then fixed with osmium tetroxide. Thick sections stained with 1% toluidine blue were used to identify the area of interest, and ultra thin sections (70 nm) were used for examination after staining with uranyl acetate and lead citrate.

Immunoblotting analysis and quantification

The uncropped blots corresponding to those presented in the Figures of the main article are shown in Figure S13. Homogenates for western blot analyses were obtained from either the liver samples or cell cultures. The proteins were resolved in 8% or 14% polyacrylamide gels by SDS-PAGE and transferred to polyvinylidene difluoride or nitrocellulose membranes (Thermo Fisher, Barcelona, Spain). The sources and dilutions of the primary and secondary antibodies may be found in Table S7. The immunoreactive bands were visualised using the SuperSignal West Femto chemiluminescent substrate (Pierce, Rockford, IL, USA), and the analysis was performed with a ChemiDoc system (Bio-Rad Laboratories, Madrid, Spain). Fumarylacetoacetate hydrolase (FAH) is used as a loading control. The bands were analysed and quantified using Image Lab 2.0 software (Bio-Rad Laboratories). All WB quantifications were normalized with the housekeeping FAH or by the ratio of total protein vs. phosphorylated protein. Phosphorylated proteins (pAKT, pAMPK, pMTOR, pS6k, and pS6) were developed and then stripped to determine total proteins. To remove primary and secondary antibodies we used 62.5 mM Tris-HCl, pH 6.7 buffer with 100 mM b-mercaptoethanol, and 2% SDS. We incubated 15 minutes at 50°C and then we washed the membranes with TBST 5 minutes 10 times before blocking.

Immunocytochemistry

After the deparaffinisation and rehydration of the liver sections, the antigens were retrieved in 0·15 M sodium citrate buffer at pH 6 in a microwave oven up to 90°C. Immunocytochemistry was performed using antibodies against 4-hydroxy-2-nonenal and paraoxonase-1. The cells stained for specific markers were quantified using ImageJ software (National Institutes of Health, Bethesda, MD, USA). The percentage of apoptotic nuclei in liver biopsies was determined by a colorimetric terminal deoxynucleotidyl transferase-mediated dUTP nick end labelling (TUNEL) assay (Click-iT™ TUNEL, Invitrogen, Thermo Fisher, Waltham, MA, USA) according to the manufacturer's instructions.

Quantitative targeted metabolomics platforms

To measure the metabolites from energy metabolism, we used a 7890A gas chromatograph coupled with an electron impact source to a 7200-quadrupole time-of-flight mass spectrometer (Agilent Technologies, Santa Clara, USA). The analysis of metabolites from one-carbon metabolism was performed with an ultrahigh-pressure liquid chromatography-quadrupole time-of-flight mass spectrometer (Agilent Technologies). Liquid chromatography was also used in separate analyses to quantify the amounts of guanine, 5-methylcytosine and 5-hydroxymethylcytosine.

DNA and RNA isolation

DNA and RNA were isolated according to the instructions of the Qiagen QIAmp DNA Micro Kit and the Qiagen RNeasy Lipid Tissue Mini Kit (Werfen, Barcelona, Spain), respectively. The concentrations of DNA and RNA were determined using a NanoDrop ND-1000 spectrophotometer (Nanodrop Technologies Inc., Wilmington, NC). The RNA integrity number (score > 8) was assessed using an RNA2100 Bioanalyser (Agilent Technologies, Santa Clara, CA) with the RNA 6000 Nano Kit.

Quantitative real-time PCR

RNA was reverse-transcribed into cDNA using the Reverse Transcription System (Applied Biosystems, Foster City, CA). Quantitative gene expression analyses were conducted on a 7900HT Fast Real-Time PCR System using the reagents provided by the respective TaqMan® Gene Expression Assays (Applied Biosystems) indicated in Table S8. All the measurements were normalised to the expression of the housekeeping gene 18S using standard procedures.

Microarray-based DNA methylation analysis

The samples included in the study were fresh-frozen human livers. DNA extraction, bisulfite conversion, site-specific oxidation and array hybridisation to the 850K microarrays was performed with Infinium human methylation EPIC beadchip array technology according to the manufacturer's instructions (Illumina, San Diego, CA).

Microarray-based gene expression analysis

One hundred nanograms of total RNA purified from the livers was used to produce cyanine 3-CTP-labeled cRNA using the Quick Amp Labeling kit, and 3 µg of labelled cRNA was hybridised to the Sureprint G3 human gene expression 8x60k v2 microarray according to the manufacturer's protocol (Agilent, Palo Alto, CA). The arrays were scanned in an Agilent Microarray Scanner, and the raw data were extracted using Agilent Feature Extraction 10.7.3.1.

Cell culture and flow cytometry analysis

HepG2 cells were obtained from ATTC and grown in high-glucose DMEM (GIBCO) supplemented with 10% fetal bovine serum, 2 mM glutamine, 1% penicillin and streptomycin and nonessential amino acids at 37°C in a humidified atmosphere with 5% CO₂. The experiments were performed by adding permeable α-KG (dimethyl-α-ketoglutarate; DMKG) at final concentrations ranging from 0.1 to 2 mM for 72 h and/or metformin at a final concentration of 10 mM. To estimate the percentage of cell death, the cells were detached and mixed with trypan blue to be analysed using the TC20 automated cell counter (Bio-Rad) according to the manufacturer's instructions. After the respective treatments, the cells were either washed two times with phosphate-buffered saline (PBS) and stored at -80°C until the extraction and quantification of metabolites or, for immunoblot assays, the media were replaced with RIPA buffer containing protease and phosphatase inhibitors (P8340, P0044 from Sigma). When required, the cells were stained with annexin V and

propidium iodide for analysis using a BD FACSCanto BD-Biosciences flow cytometer, and the data were assessed using the free software Flowing.

Primary hepatocyte isolation

Primary hepatocytes were isolated from the livers of 5-month-old wild type C57BL/6 J male mice as described.⁴ In brief, livers were perfused with Hank's Balanced Salt Solution (Invitrogen) containing 5 mM glucose supplemented with 0.5 mM EGTA and 25 mM HEPES (pH 7.4 at 37°C) using a CTP100 peristaltic pump (ThermoFisher). After exsanguination of the liver, perfusion was changed to DMEM (Sigma-Aldrich D5546) supplemented with 100 U/mL Penicillin and 0.1 mg/mL Streptomycin (Pen/Strep), 15 mM HEPES, and 100 U/mL of collagenase (Type IV, Worthington). Then cells were liberated and cell suspension was then filtered through a 70 µM cell strainer and centrifuged at 50 g x 2 min 3 times. Following centrifugation, cell pellets were resuspended in DMEM (Sigma-Aldrich D5796) supplemented with Pen/Strep, 5 mM HEPES, 10 nM dexamethasone, and seeded into 6-well plates or 24-well Seahorse plates precoated with collagen I (Sigma-Aldrich). One hour later the media was changed to DMEM (Sigma-Aldrich D5546) supplemented with Pen/Strep, 5 mM HEPES, 10 nM dexamethasone and 10% FBS. Media was changed 3 h later to serum-free Earl's balanced salts (Sigma-Aldrich E2888) supplemented with Pen/Strep, 5 mM HEPES, 10 nM dexamethasone, glucose (1,75 g/l) and sodium pyruvate (1mM), treated or not with metformin and/or DMKG. Cells were cultured for 38 hours for various experiments. After 38 hours of culture, hepatocytes were frozen in liquid nitrogen and lysed in RIA assay buffer (20 mM Tris-HCl (pH 7.5), 150 mM NaCl, 1 mM Na2EDTA, 1 mM EGTA, 1% NP-40, 1% sodium deoxycholate) with protease and phosphatase inhibitors P0044, P5725 and P8340.

Oxygen consumption and ECAR

Mitochondrial bioenergetics of primary hepatocytes was measured using an XF24 Extracellular Flux Analyzer (Agilent).⁵ After 38 hours of culture, cells were washed with Seahorse assay media (Seahorse Bioscience). Plates were incubated in a CO₂-free incubator at 37 °C for 1 h to allow temperature and pH equilibration, after which oxygen consumption rate (OCR) was measured in the XF24 Extracellular Flux Analyzer over a period of 88 min. Mitochondrial processes were examined through sequential injections of oligomycin (4 µM) at min 27, carbonyl cyanide 4-(trifluoromethoxy) phenylhydrazone (FCCP; 2 µM) at min 52, rotenone (1µM) at min 78, and antimycin A (5 µM) at min 104. ECAR was determined under basal culture conditions.

Bioinformatics

To analyse the gene expression microarray, spot signals were normalised with Agilent Gene Spring GX v14.8 software and filtered to keep only the autosomal genes for further comparisons (20,214 genes) in R. Using the t.test function, we determined significance of expression difference between NASH and Non-NASH patients (n = 8 each). We determined 345 genes to have p < 0.05 and log₂(NASH/Non-NASH) > 1. All RNA expression data were used for the integration of DNA methylation and gene expression data (see below). For the DNA methylation array, the raw data were analysed using the minfi package in R with annotations from Illumina Human Methylation EPICmanifest v0.3.0 and Illumina Human Methylation EPICanno.ilm10b2.hg19 v0.6.0. The data were normalised and filtered to keep only the autosomal CpGs using the preprocess Quantile function with mergeManifest=T and dropLociWithSnps() with snps=c("SBE", "CpG", "Probe") and maf=0 parameters. Each CpG has a beta value (calculated using getBeta), which is the fraction of methylated / methylated + unmethylated signal, bound between 0 and 1. We performed Wilcoxon rank-sum tests on each CpG (n = 8 for each group) to determine significant differences. We also determined the average beta level in NASH and Non-NASH patients and then retained the CpGs whose average Δ beta > 0.05 and whose p-value < 0.05 as significantly differentially methylated. Subsets of CpGs across features of the genome were annotated using the genomatome package with hg19 knownGene files downloaded from the UCSC Table Browser, as described. The gplots package was used for heatmap visualisation. To assess the relationship between CpG methylation and gene expression, we merged the differentially methylated CpGs in gene promoters with the RNA microarray data and correlated beta and expression values. *Circos* visualization

was generated using the *circlize* package. Kyoto Encyclopedia of Genes and Genome (KEGG) pathway analysis of selected genes subsets was performed.

References

1. Aranda N, Viteri FE, Montserrat C, Arija V. Effects of C282Y, H63D, and S65C HFE gene mutations, diet, and life-style factors on iron status in a general Mediterranean population from Tarragona, Spain. *Ann Hematol* 2010; **89**: 767–73
2. Mechanick JI, Apovian C, Brethauer S, Garvey WT, Joffe AM, Kim J, et al. Clinical practice guidelines for the perioperative nutrition, metabolic, and nonsurgical support of patients undergoing bariatric procedures. *Surg Obes Relat Dis* 2020; **16**: 175–247
3. Vives M, Molina A, Danús M, Rebenaque E, Blanco S, París M, et al. Analysis of gastric physiology after laparoscopic sleeve gastrectomy (LSG) with or without antral preservation in relation to metabolic response: a randomised study. *Obes Surg* 2017; **27**: 2836–2844
4. Zhang W, Sargis RM, Volden PA, Carmean CM, Sun XJ, Brady MJ. PCB 126 and other dioxin-like PCBs specifically suppress hepatic PEPCK expression via the aryl hydrocarbon receptor. *PLoS One* 2012; **7**: e37103.
5. Qiao A, Jin X, Pang J, Moskophidis D, Mivechi NF. The transcriptional regulator of the chaperone response HSF1 controls hepatic bioenergetics and protein homeostasis. *J Cell Biol* 2017; **216**:723–741